NO_2 Air Pollution Trends and Settlement Growth in Megacities

Thilo Erbertseder, Hannes Taubenböck, Thomas Esch, Lorenza Gilardi, Heiko Paeth, and Stefan Dech

***Abstract*—Megacities exert substantial demands on the world's energy resources, thereby producing large shares of atmospheric emissions and air pollution. Despite several studies on nitrogen dioxide (NO_2) changes in megacities, a systematic analysis in relation to settlement growth is still pending. This study examines the trends of tropospheric NO_2 pollution in 38 megacities regarding settlement growth by analyzing Earth Observation data. Multiannual records of tropospheric NO_2 from Global Ozone Monitoring Experiment (GOME), Scanning Imaging Absorption Spectrometer for Atmospheric Chartography, GOME-2A, and GOME-2B are evaluated regarding the World Settlement Footprint evolution from 1996 to 2015. Compared to previous studies, this work strictly uses remote sensing data and the spatial concept of functional urban areas. Therefore, uncertainties due to inconsistent spatial references, incomparable administrative units, as well as heterogeneously reported local data are widely excluded to enable an appropriate comparison of megacities across the globe. On average, we observe an increase in tropospheric NO_2 burden of 5.06 $\pm$ 0.83%/year and a relative settlement growth of 2.87%/year for the time period considered. We find a wide range of trends: relative NO_2 pollution ranges from an increase of 44.0 $\pm$ 5.9%/year to a decrease of -3.2 ± 0.2%/year, settlement growth rates vary from 0.3%/year to 9.5%/year. Despite this variety, the results exhibit a pronounced relation to the income group following the world's economies classification of the World Bank. Complemented by a cluster analysis and ranking of the megacities, the study provides indicators to develop a better understanding of the drivers and impacts of urbanization and air pollution.**

***Index Terms*—Air pollution, income class, megacities, nitrogen dioxide (NO_2), time series analysis, urban growth, urbanization.**

Manuscript received 12 March 2024; revised 13 May 2024; accepted 18 June 2024. Date of publication 26 June 2024; date of current version 12 July 2024. This work was supported in part by the European Union's Horizon 2020 project e-shape under Grant 820852 and in part by the German Federal Ministry of Education and Research (BMBF) within Urban Climate Under Change [UC]^2 under Grant 01LP1602P. *(Corresponding author: Thilo Erbertseder.)*

Thilo Erbertseder and Lorenza Gilardi are with the German Remote Sensing Data Center, German Aerospace Center (DLR), 82234 Wessling, Germany (e-mail: thilo.erbertseder@dlr.de; lorenza.gilardi@dlr.de).

Hannes Taubenböck and Stefan Dech are with the German Remote Sensing Data Center, German Aerospace Center (DLR), 82234 Wessling, Germany, and also with the Institute for Geography and Geology, University of Würzburg, 97074 Würzburg, Germany (e-mail: hannes.taubenboeck@dlr.de; stefan.dech@dlr.de).

Thomas Esch is with the German Remote Sensing Data Center, German Aerospace Center (DLR), 82234 Wessling, Germany, and also with the Faculty of Geomatics, Computer Science and Mathematics, Stuttgart University of Applied Sciences, 70174 Stuttgart, Germany (e-mail: thomas.esch@dlr.de).

Heiko Paeth is with the Institute for Geography and Geology, University of Würzburg, 97074 Würzburg, Germany (e-mail: heiko.paeth@uni-wuerzburg.de).

Digital Object Identifier 10.1109/JSTARS.2024.3419573

I. Introduction

ACCORDING to the World Health Organization (WHO), air pollution is now considered the largest single environmental health risk [1]. Humans are exposed daily to a variety of environmental stressors, such as nitrogen dioxide (NO_2), ozone (O_3), and particulate matter (PM), to name a few. These can lead to a wide spectrum of adverse health effects ranging from cardiovascular, respiratory, and metabolic diseases to susceptibility to infectious diseases, such as influenza or COVID-19 [2], [3], [4], [5]. A recent study showed that an average of 2.9 years of life expectancy is lost worldwide due to (outdoor) air pollution [6]. Around 99% of the global population is exposed to air pollutant levels that exceed the WHO guideline limits, with low- and middle-income countries suffering from the highest exposures [1].

Although air pollution is a challenge of global importance, exposure to air pollutants is predominantly an urban threat [2]. Urban areas across the globe account for less than 2% of the land surface only; however, they have always been spatial focal points of air pollution and resource needs as they consume two-thirds of the global energy with a majority of fossil fuels [7].

The rise in the world's urban population over the past few decades has led to an increase in the number of megacities, generally defined as cities with a population of greater than 10 million [8]. As such, megacities have become global centers of population growth, settlement growth, production, energy demand, and as a consequence emission of greenhouse gases, air pollutants, and their precursor substances [9]. As these cities continue to grow [10], emissions are a concern, not only for local air quality but also for regional and continental scales and even for global climate, due to interactions with processes linked to climate change, such as radiative forcing [11], [12]. Evaluating past air pollutant trends in urban areas gives insight into the effectiveness of previous and current policies to curb emissions and control these levels, and possibly supports measures for future policies [13].

This study focuses on the air pollutant NO_2 as it can be attributed mainly to anthropogenic combustion processes associated with transport, industry, energy production, and heating [9]. Due to its short lifetime in the lowermost troposphere during daytime (2–8 h), it predominantly remains at the emission sources and its amount is sensitive to emission changes [14], [15]. NO_2 is a regulated air pollutant and directives demand routine monitoring by ground-based stations in ambient air. However, the global availability of these measurements is heterogenous, the spatial representativity of point measurements

for large urban landscapes is limited, and such data is often scarce in the Global South. Since 1995, space-based observation of the tropospheric composition has enabled operational daily monitoring of NO_2 levels on a global scale [16]. Contrary to in-situ measurements, space-based observations are gathered homogeneously with the same instrument and are sampled on a consistent and spatially integrating grid [17]. However, these differ from in-situ measurements at ground level as they yield indirect measurements of vertically integrated quantities, such as tropospheric NO_2 column densities [18], [19].

Due to the short lifetime of NO_2 and its predominantly human origin from combustion processes, as outlined above, tropospheric NO_2 constitutes an invaluable tracer to examine the anthropogenic footprint in the troposphere as well as human activity in different geographic perspectives and scales [17], [20], [21], [22]. Since natural contributions to the tropospheric NO_2 burden are small and are confined to lightning [23] and microbial processes in soils [24], it has been used to delineate urban pollution islands and pollution hotspots [20], [22], [25] and to reveal weekly cycles reflecting anthropogenic activity patterns in urban environments [21], [26], [27]. Furthermore, tropospheric NO_2 column densities have been extensively used to infer NO_x emissions, see, e.g., [15], [28], [29], and [30].

Several satellite-based studies analyzed NO_2 changes and trends in selected regions or megacities by examining multi-annual records from a single sensor or a multisensor approach. In the first study, Richter et al. [31] performed a linear regression of tropospheric NO_2 annual means from the Global Ozone Monitoring Experiment (GOME) [16] for several regions in the world. A detailed analysis on NO_2 trends over China combining data from GOME and the SCanning Imaging Absorption spectroMeter for Atmospheric ChartographY (SCIAMACHY) [32] was published by van der A et al. [33]. They used the time series analysis approach of Weatherhead et al. [34] in a simplified way to detect trends in monthly mean data and to examine their significance. For a selection of megacities and urban agglomerations, NO_2 trends were derived from single-sensor data records using the same time series analysis method by Schneider and van der A [35] and Schneider et al. [36], while Konovalov et al. [37] applied a nonlinear trend fitting and Geddes et al. [38] used least-squares linear regression. Finally, the combination of data records from different sensors enabled the generation of longer times series and the detection of robust trends [39] and even trend reversals [40].

However, the derived trends in all these studies have so far neither been related to consistent spatial units like functional [41] or morphological urban areas [42], nor sufficiently to socioeconomic status or demographic parameters. This limits the interpretation of the findings and the reliability of a global comparison of cities. In previous studies, the derived trends are often related to a city or megacity, but no transparent spatial delineation is defined [39], [40]. Whether the observed mean or trend refers solely to the city center or to a grid cell covering the urban area and its surroundings becomes increasingly important as cities grow in size. It is inevitable to define a spatial unit for geographic comparisons, in particular, for such large agglomerations, such as megacities or megaregions [17], [43]. In addition, interpreting trends alone might result in ambiguous conclusions. On the one hand, a decreasing trend in NO_2 could result from a decline in population or traffic, reduced production or wealth. On the other hand, it could result from a transition to a green economy or energy and the implementation of new measures mitigating emissions like the introduction of new filtering techniques or electromobility, to name a few. Beyond that, population numbers or the gross domestic product (GDP) generally refer to administrative units leading to inconsistent spatial delineations of cities introducing bias in comparisons across cities [42]. In addition, they strongly vary in quality depending on the country and result in heterogenous datasets for comparisons of cities across the globe. As such, these numbers, concepts, and findings are prone to large uncertainties.

Therefore, a global objective and consistent measure from Earth Observation (EO) data are required. The World Settlement Footprint (WSF) [44] is derived from satellite data and exhibits an objective and multitemporal estimate of settlement growth that is considered a proxy for urbanization and economic development in this work. EO has proven to be an effective instrument, in particular, with respect to large-scale mapping of human settlements, such as megacities at continental and global scales [10], [45]. The WSF evolution [46] that is available yearly from 1985 to 2015 provides an essential component to develop a better understanding of the drivers and impacts of urbanization and air pollution [47]. A first attempt to link the settlement footprint to NO_2 trends was made by Erbertseder et al. [48].

Against this background, this study centers on a systematic analysis of 38 megacities across the globe in relation to NO_2 pollution trends and settlement growth from 1996 to 2015. The study purely relies on satellite-based EO data. To overcome the problem of missing and heterogeneously defined spatial units, these data are rigorously analyzed with respect to functional urban areas (FUA) that provide a delineation of the cities based on principles of urban economics [41]. Furthermore, the results are ranked, classified, and interpreted regarding the income groups according to the world's economies classification of the World Bank [49]. The study aims at drawing overarching conclusions concerning the full spectrum of megacities, encompassing aspects, such as anthropogenic pollution and settlement growth, serving as a proxy for both urbanization and economic development. In addition, it will facilitate an analysis of their transformative stages, including transitions toward environmental sustainability (green transition), and their position within the global economic landscape.

The rest of this article is organized as follows. Section II describes the study area and the datasets used, followed by Section III outlining the methodology. Sections IV and V present the results and discussion including strengths, limitations, and perspectives of the work. Finally, Section VI concludes this article.

II. Study Area and Data

A. Functional Urban Areas

Instead of conventional, but heterogeneously defined administrative city units or arbitrarily chosen grid cells or geographic domains, we apply the concept of FUAs. This approach enables us to consistently delineate megacity areas and megaregions

against their rural surroundings and to define their spatial extent and urban pollution island. An FUA is defined by aspects of urban economics and consists of a city and its commuting zone, where the latter represents the area of influence of the city in terms of labor market flows. The Organization for Economic Co-operation and Development defines an FUA as the union of the administrative units in which at least 15% of the population is commuting to the main urban center of the area. To improve international comparability of urban-related statistics and indicators with an explicit spatial dimension, this method was developed further to estimate the number and extent of FUAs worldwide based on objective characteristics [41]. The improved method does neither rely on information on local unit boundaries nor data on commuting flows, which are usually unavailable in most countries. The FUAs are estimated through an automated classification procedure based on uniformly measurable parameters, such as travel time from urban centers, area of urban centers, local population, and country GDP per capita. These classification results are available as the Global Human Settlement Functional Urban Area (GHS-FUA) layer. To be consistent with the other datasets in this study, we apply the GHS_FUA_UCDB2015_GLOBE_R2019A dataset for the reference year 2015[1] [50]. These FUAs, defined as polygon for each megacity, are used consistently throughout the study for any spatial aggregation.

B. Megacities

Megacities are defined by the United Nations (UN) as a conurbation or metropolitan area with a population exceeding 10 million inhabitants [8]. This study comprises 38 megacities across the globe referring to the baseline year 2015 (see Table I). By means of the World Urbanization Prospects, the Population Division of the UN provides time series of the population of the largest 30 cities or cities with over 300k inhabitants and their population [8]. However, as can be inferred from Table I, the megacities examined in this study primarily follow the ranking of the largest cities with respect to the population of the FUAs. A previous study has substantiated that a global ranking of the largest cities is a challenging task [42]. This is evident by the differing population numbers given by the UN and GHS-FUA depending on the administrative areas under consideration. The list of megacities in this article includes the 30 cities with the largest population in 2015 regarding the FUAs of the Global Human Settlement Layer [50] and the 30 largest cities in the world as of 2015 according to the UN [8]. As such, the list can be considered as a representative selection of megacities and a valid combination of these two datasets. However, only the population numbers of the FUAs are considered in any further analysis here.

C. NO_2 Pollution

Global observations of the tropospheric NO_2 burden are derived from GOME (1996–2003) [16], SCIAMACHY (2002–2012) [32], and GOME-2A and GOME-2B (2007–2015; 2013–2015) [51]. These instruments are nadir-scanning spectrometers that orbit in a polar Sun-synchronous pattern with a fixed equator crossing time. The spectrometers are passive and sense backscattered solar radiation from the Earth's atmosphere and surface as well as extraterrestrial solar irradiance ranging from the ultraviolet to the visible and near-infrared portion of the spectrum at a high spectral resolution of less than 0.5 nm. The retrieval algorithm for NO_2 is based on the Differential Optical Absorption Spectroscopy (DOAS) technique exploiting the wavelength range from 405 to 465 nm. This method is utilized to derive the total slant column of NO_2 from the radiance spectra measured by the instrument. By applying the Beer–Lambert law, the DOAS fitting procedure entails a least-squares inversion aimed at isolating absorption signatures attributable to trace gases from the influence of broadband background processes, such as extinction arising from scattering on molecules and aerosols. In the next step, the total slant column density of NO_2 is converted into a vertical column density. After separating the stratospheric NO_2 contribution from the total vertical column, the resulting tropospheric residue can finally be converted into the tropospheric NO_2 vertical column density by applying the ratio of stratospheric and tropospheric air mass factors. The NO_2 content is finally given as the number of molecules per area (molecules /cm^2), mol per area (mol/m^2), or area-related mass (μg/m^2).

To combine the tropospheric NO_2 observations given the different sensor and orbit characteristics, a methodology was developed in [39]. The approach was applied Georgoulias et al. [40] to gain a self-consistent dataset of monthly mean values on a regular grid of $0.25° \times 0.25°$ spatial resolution. This study is based on the dataset of [40] as provided by www.temis.nl. To be consistent with the other data sources of the study, the time period considered covers 1996–2015.

D. Settlement Footprint

To track the rapid urbanization observed in the recent past, yearly high-resolution settlement footprint data are a prerequisite for any further analysis. The settlement growth of the megacities under consideration is, therefore, derived from the WSF [44]. It comprises a binary mask outlining the extent of human settlements worldwide. In particular, the WSF evolution dataset is used to outline the global human settlement extent at a 30 m spatial resolution on a yearly basis from 1985 to 2015 [46].

The classification was performed on the Google Earth Engine platform using the complete record of Landsat imagery. For each year, all available Landsat-5 and −7 scenes that were acquired over a given area of interest were gathered. After performing cloud and cloud-shadow masking, spectral indices were derived. Among others, these include the normalized difference built-up index, normalized difference vegetation index, and modified normalized difference water index. In the next step, key statistics were calculated, including temporal mean, standard deviation, minimum, and maximum. Temporal features prove generally robust if computed over at least seven clear cloud-/cloud-shadow-free observations. Accordingly, if this constraint was not satisfied for a given pixel in the target year, the time

[1] [Online]. Available: https://ghsl.jrc.ec.europa.eu/ghs_fua.php

TABLE I
LIST OF THE 38 MEGACITIES EXAMINED IN THE STUDY, SORTED IN DESCENDING ORDER BY THE POPULATION OF THE FUAS IN THE YEAR 2015 [8], [50]

Rank	Megacity	Country	Latitude [°N]	Longitude [°E]	Population FUA 2015 [Mio.]	Population UN 2015 [Mio.]	Area FUA 2015 [km²]
1	Guangzhou	China	23.1255	113.2574	45.64	11.69	12 567
2	Jakarta	Indonesia	-6.2118	106.8416	39.81	10.17	9601
3	Tokyo	Japan	35.6895	139.6917	36.47	37.26	11 971
4	Delhi	India	28.6667	77.2167	30.08	25.87	5569
5	Shanghai	China	31.2222	121.4581	26.92	23.48	5878
6	Dhaka	Bangladesh	23.7104	90.4074	26.74	17.60	5760
7	Manila	Philippines	14.6042	120.9822	24.96	12.86	4873
8	Kolkata	India	22.5335	88.3560	24.64	14.42	5237
9	Seoul	South Korea	37.5683	126.9778	24.29	9.90	7053
10	Cairo	Egypt	30.0392	31.2394	23.49	18.82	4348
11	Mumbai	India	19.0740	72.8808	22.28	19.32	2367
12	São Paulo	Brazil	-23.5475	-46.6361	21.68	20.88	6077
13	Mexico City	Mexico	19.4273	-99.1419	21.41	21.34	4831
14	Beijing	China	39.9075	116.3972	21.28	18.42	5536
15	New York	USA	40.7170	-74.0037	19.52	18.65	17 489
16	Osaka	Japan	34.6758	135.5538	17.62	19.30	10 090
17	Moscow	Russia	55.7550	37.6218	16.38	12.05	8459
18	Bangkok	Thailand	13.7220	100.5252	16.29	9.40	5161
19	Los Angeles	USA	34.0317	-118.2417	15.66	12.35	10 407
20	Buenos Aires	Argentina	-34.6051	-58.4004	14.98	14.71	5376
21	Istanbul	Türkiye	41.0138	28.9497	14.79	14.13	2540
22	Karachi	Pakistan	24.9056	67.0822	13.42	14.29	1348
23	Tehran	Iran	35.6944	51.4215	13.41	8.55	3332
24	Ho Chi Minh City	Vietnam	10.7500	106.6667	12.83	7.35	3036
25	Jieyang	China	23.5526	116.3721	12.66	0.91	5922
26	London	U.K.	51.5085	-0.1257	12.60	8.66	6605
27	Lagos	Nigeria	6.4531	3.3958	12.34	12.24	2284
28	Bengaluru	India	12.9719	77.5937	11.93	10.14	2054
29	Lahore	Pakistan	31.5497	74.3436	11.79	10.37	3154
30	Chengdu	China	30.6667	104.0667	11.75	8.36	4034
31	Paris	France	48.8534	2.3488	11.24	10.73	6778
32	Rio de Janeiro	Brazil	-22.9028	-43.2075	10.81	12.94	3598
33	Lima	Peru	-12.0432	-77.0282	9.67	9.81	2121
34	Chicago	USA	41.8500	-87.6501	8.80	8.77	13 185
35	Wuhan	China	30.5833	114.2667	8.53	7.90	26 821
36	Tianjin	China	39.1088	117.1886	8.32	12.52	2413
37	Chongqing	China	29.5628	106.5528	6.04	13.37	2267
38	Kinshasa	Democratic Republic of the Congo	-4.3276	15.3136	5.76	11.60	591

frame was enlarged backward until the condition was met. The WSF data are available via the DLR EOC Geoservice.[2]

E. Income Group

The World Bank Group assigns the world's economies to four income groups—low, lower-middle, upper-middle, and high [49], [52]. The classifications are updated each year on 1 July, based on the gross national income (GNI) per capita of the previous calendar year. GNI measures are expressed in U.S. dollars using conversion factors derived according to the Atlas method, which in its current form was introduced in 1989. The World Bank's income classification aims to reflect a country's level of development, drawing on Atlas GNI per capita as a broadly available indicator of economic capacity.

III. METHODOLOGY

A. Conceptualization

The study aims at analyzing, ranking, and classifying megacities with respect to NO_2 air pollution and settlement growth and to examine their statistical relationship. The conceptualization

[2][Online]. Available: https://download.geoservice.dlr.de/WSF_EVO

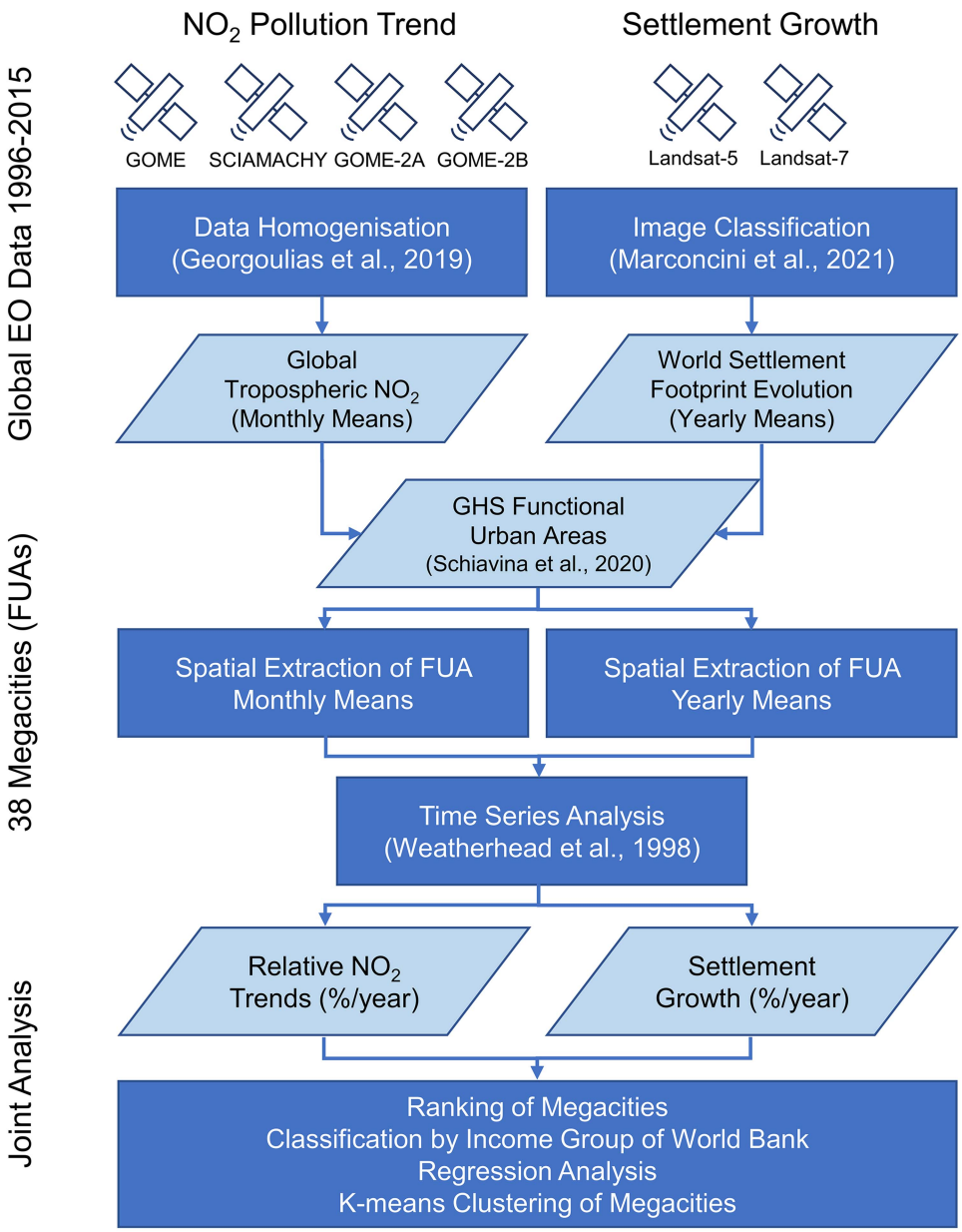

Fig. 1. Conceptualization of the methodology.

and methodology are illustrated in Fig. 1 and can be summarized as follows.

The first step to achieve these objectives is the exploitation of globally consistent satellite-based long-term records of tropospheric NO_2 (see Section II-C) and the settlement footprint (see Section II-D) from 1996 to 2015.

Second, the FUAs (see Section II-A) for the 38 megacities (see Section II-B) and the epoch of 2015 were derived from the GHSL_FUA and represented by polygons in shapefiles. Consistently, additional urban parameters, such as population or area size of the FUAs, were extracted.

Third, the time series of tropospheric NO_2 was extracted for each megacity's FUA. Therefore, all the monthly means were oversampled on a $0.01 \times 0.01°$ grid without any interpolation. For each megacity and month, an FUA-weighted statistic was calculated, including mean, minimum, maximum, standard deviation, number of pixels, and number of missing values as a consequence of cloud cover in the corresponding month.

Fourth, the settlement footprint, i.e., WSF evolution data, was extracted for each megacity within the corresponding FUA and time period on a yearly basis (see Section III-C).

Fifth, the analysis of the resulting time series and the separation of the linear trend component were performed by time series decomposition, as described in Section III-B. The absolute and relative settlement growth rates were derived based on the statistical moments of the settlement area increments.

Sixth, the megacities were systematically analyzed and ranked according to the relative tropospheric NO_2 trends (%/year) and the relative settlement growth (%/year). The megacities were further examined regarding the per capita pollution and the

income group following the world's economies classification of the World Bank (see Section II-E).

Seventh, by means of regression analysis, the hypothesis was tested whether there is a statistical relationship between relative NO_2 trends and relative settlement growth in megacities (both in %/year).

Finally, the spectrum of megacities was analyzed by k-means clustering to yield a classification of the megacities with respect to NO_2 air pollution and settlement growth (see Section III-D). Can we identify groups of megacities that evolve similarly? Which megacities exhibit strong settlement growth while reducing the overall NO_2 burden by implementing measures of green transition?

The method proposed in this study will enable us to derive general conclusions for the entire range of megacities, regarding urbanization and settlement growth, their transformative stages toward environmental sustainability, and their positioning in the world economies.

B. Time Series Analysis of NO_2 Data

Based on the satellite long-term records of tropospheric NO_2 (see Section II-C), a time series analysis with a multicomponent model [34] was applied to identify linear trends of NO_2 and their uncertainties in megacities. This approach has been widely used to model geophysical quantities and, in particular, monthly means of observed tropospheric NO_2 vertical column densities Y as a function of time t [33], [39], [40], [53]

$$Yt = \mu + S_t + \frac{1}{12}\omega + N_t \tag{1}$$

where μ is a constant term, S_t is the seasonal component, ω represents the linear trend per year, and N_t is the residual variability. The seasonal component is modeled as a sinusoidal and is assumed to be stationary, i.e., invariant in time

$$\mathrm{S}_t = \sum_{J=1}^{4}\left[\beta_{1,j}\sin\left(\frac{2\pi jt}{12}\right) + \beta_{2,j}\cos\left(\frac{2\pi jt}{12}\right)\right] \tag{2}$$

where eight superimposed harmonics are fitted by the coefficients $\beta_{1,1}$–$\beta_{2,4}$. For the unexplained part of the time series, the noise N_t is considered to be autoregressive of the order of 1, i.e.,

$$N_t = \varphi N_{t-1} + \varepsilon_t \tag{3}$$

where ε_t are independent random variables and φ is the first-order autocorrelation of the noise among successive monthly means, given as follows:

$$\varphi = \mathrm{Corr}(N_t; N_{t-1}) \tag{4}$$

Like the seasonal component, the noise process is assumed to be stationary with $-1<\varphi<1$. Following [34], the uncertainty of the linear trend component σ_ω can be derived as follows:

$$\sigma_\omega = \left[\frac{\sigma_r}{n^{3/2}}\sqrt{\frac{1+\varphi}{1-\varphi}}\right] \tag{5}$$

with σ_r being the standard deviation of the detrended residuals, n is the number of months considered, and φ is the first-order autocorrelation of the residuals. The significance of the linear trend ω can then be estimated at a 95% confidence level if

$$\left|\frac{\omega}{\sigma_\omega}\right| > t_\omega \tag{6}$$

where σ_ω is the uncertainty of the trend and $t_\omega$is the value of Student t-distribution for a significance level of $\alpha = 0.05$ and the degrees of freedom defined by the number of months of the times series n [54], [55]. The resulting relative trend and its uncertainty are given as percent per year (%/year).

C. Analysis of Settlement Footprint Data

Time series of the settlement area per megacity were calculated from WSF evolution data for the period 1996–2015 (see Section II-D) to match with the observation period of the NO_2 satellite data starting in 1996. In this study, we understand the terms "settlement footprint" or "urbanized areas" as the land directly occupied by a particular physical man-made structure. Thus, this definition represents a "settlement mask," defined by buildings, streets, and impervious surfaces [10]. The geographical extent of each megacity was delineated using the concept of the FUA. Consequently, the yearly growth in settlement area was calculated in km^2 in absolute terms and the relative growth rate in %/year.

D. Classification of Megacities According to Growth Dynamics and NO_2 Trends

K-means clustering is an unsupervised machine learning technique that allows the identification of clusters, i.e., similar groups of data points within the data cloud. It is the most common partitioning method for multivariate data [56].

We apply this method to gain a classification of megacities according to growth dynamics and NO_2 trends. All inputs are purely satellite-based parameters, namely, the relative tropospheric NO_2 trend (%/year), the mean NO_2 burden (10^{15} molecules/cm^2), and the relative settlement growth (%/year). These data were normalized. In order to find the optimal number of clusters, the silhouette and elbow methods were used [57]. Based on these methods, and a systematic test of various cluster numbers, five clusters were determined to be most appropriate for this study.

IV. Results

As a first illustration of the results of this study, Fig. 2 shows examples of the WSF evolution depicting the extent and yearly growth of human settlements for the megacities Chengdu, China (left column, top), Bangkok, Thailand (middle), and Lima, Peru (bottom) within their FUAs. The panels on the right display the corresponding time series of monthly mean tropospheric NO_2 from 1996 to 2015 for the related FUAs. The red line illustrates the linear trend component as a result of the time series decomposition. The related relative trends (%/year) are annotated in the panels and are all significant at the 95% confidence level for the three cities. These three examples demonstrate a quite different overall development. Chengdu shows a very dynamic settlement growth and also a very strong increase in tropospheric NO_2 of 22.05 $\pm$ 2.50%/year. Bangkok visually also reveals a

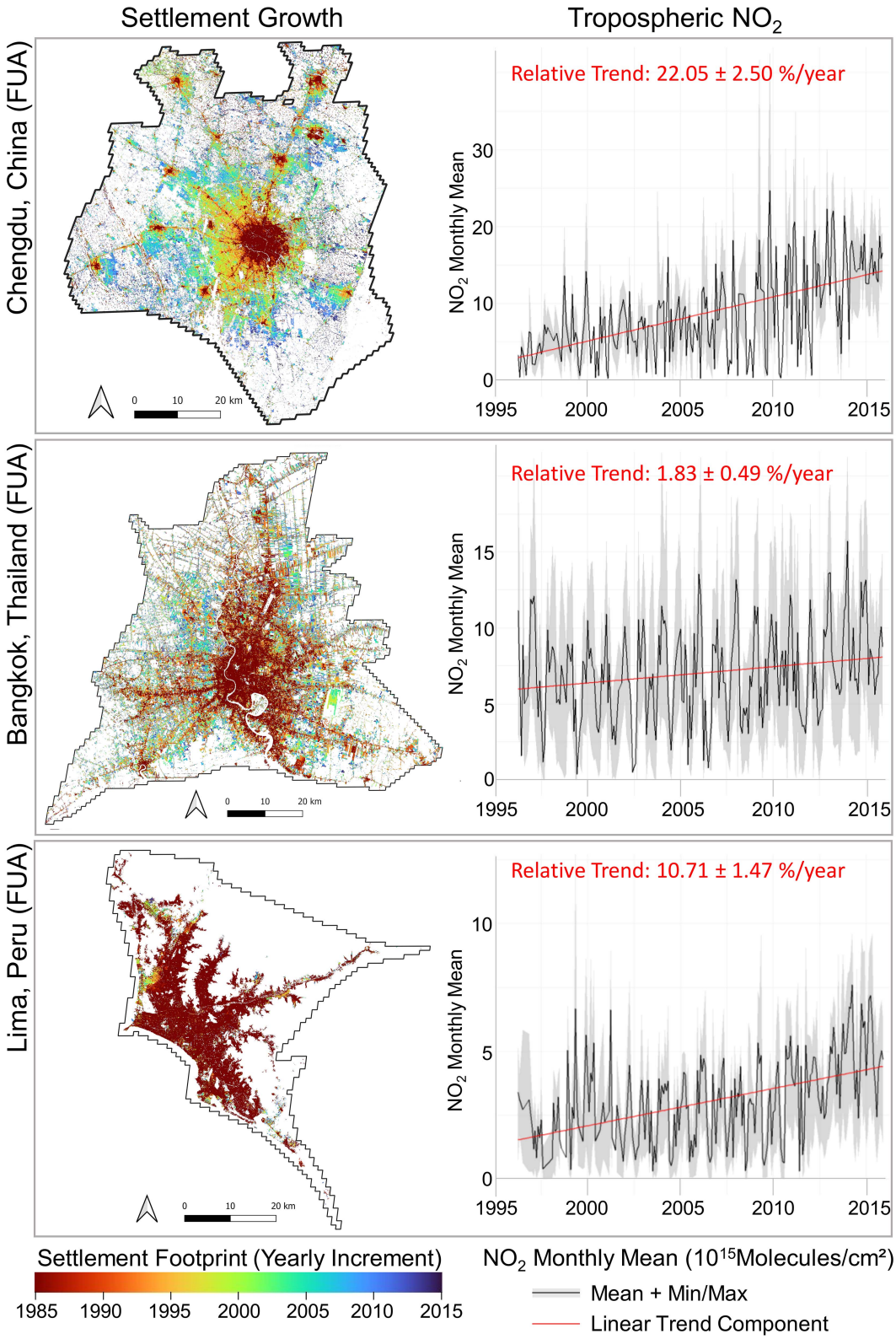

Fig. 2. Examples of the WSF evolution (left column) depicting the extent and yearly growth of human settlements from 1985 (dark red) to 2015 (dark blue) for the megacities Chengdu, China (top), Bangkok, Thailand (middle), and Lima, Peru (bottom). In the corresponding panels on the right, time series of tropospheric NO_2 from 1996 to 2015 for the related FUAs are shown. The red line illustrates the linear trend component. The relative trends are annotated in the panels.

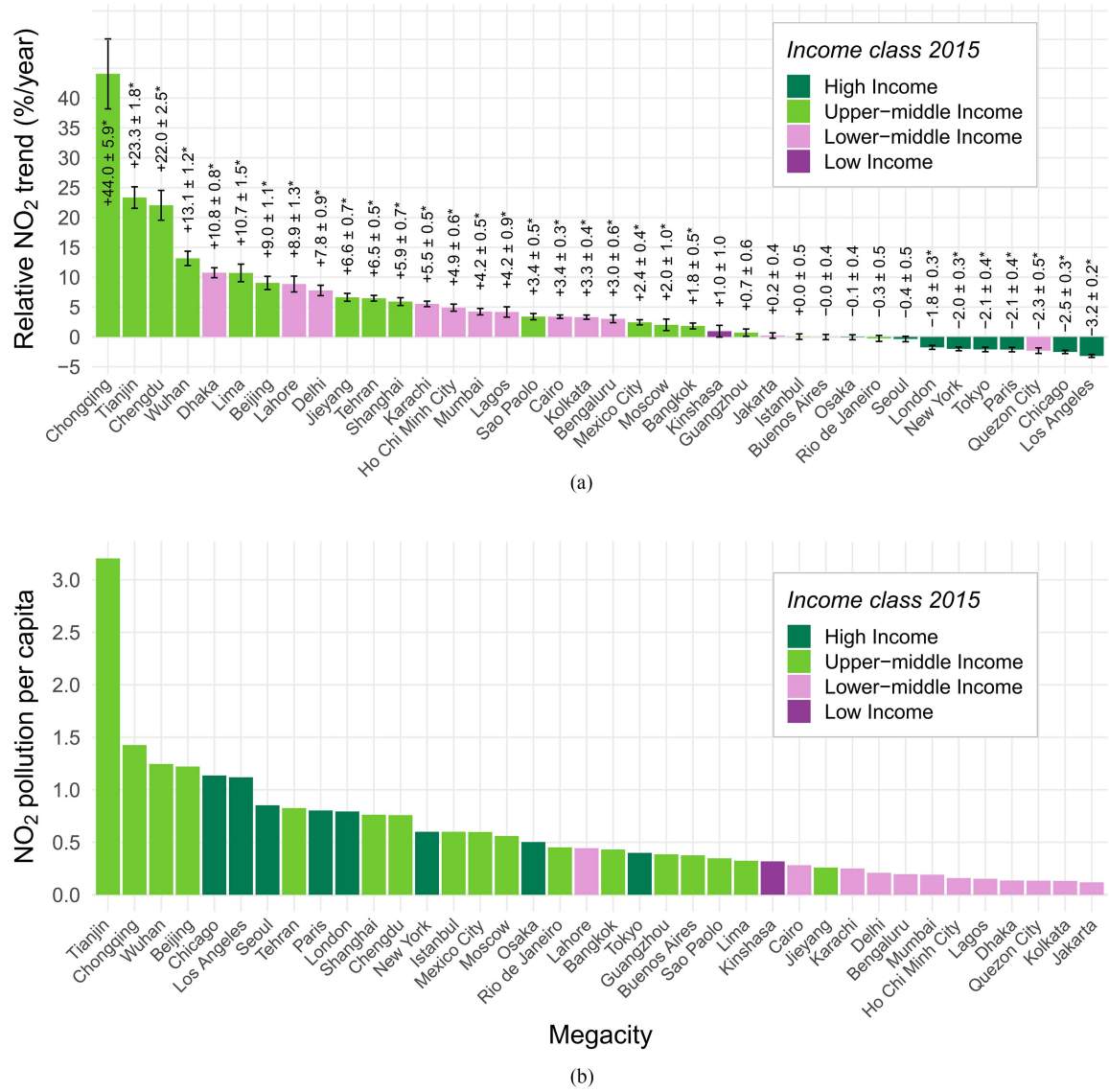

Fig. 3. (a) Relative tropospheric NO_2 trend (%/year) for each megacity FUA and the period 1996–2015, and (b) NO_2 pollution per capita for each megacity FUA and the same period expressed in (10^{15} Molecules cm^{-2} 10^6 Inhabitants^{-1}). Cities are sorted in descending order. Income groups are indicated according to the world's economies classification of the World Bank [52]. Asterisks in (a) indicate the significance of the trend at the 95% level.

relatively dynamic settlement growth, but just a weak increase in NO_2 of 1.83 ± 0.49%/year can be observed. Contrarily, Lima exhibits almost no settlement growth within this period, but a strong increase in tropospheric NO_2 pollution of 10.71 ± 1.47% year.

This diversity highlighted here asks for a more systematic analysis and presentation of the results for the 38 megacities considered. Therefore, Fig. 3(a) illustrates the full spectrum of the relative NO_2 pollution trends (%/year) sorted by magnitude. In general, we find that the trends in the examined period from 1996 to 2015 vary—from strong increases to moderate declines.

When we compare the relative NO_2 trends, the values range from an increase in Chongqing of 44.05 ± 5.86%/year to a decrease in Los Angeles of -3.19 ± 0.24%/year. The mean NO_2 trend for all the 38 megacities is 5.06 ± 0.83%/year and the median is 3.16 ± 0.51%/year.

To put the trends into a socioeconomic context, the income groups are overlaid following the world's economies classification of the World Bank [49]. It is striking to see that the strongest increases in tropospheric NO_2 pollution occur predominantly in megacities of upper middle-income countries (UMICs) (Chongqing, Tianjin, Chengdu, and Wuhan) followed by cities in lower middle-income countries (LMICs) (Dhaka, Lahore, and Delhi). Megacities in high-income countries (HICs), however, solely appear at the very right of the bar chart. They all show declining trends, i.e., improving NO_2 air quality (Los Angeles, Chicago, Paris, Tokyo, New York, London, and Seoul). The only exception is Quezon City (Manila, Philippines), which needs further clarification.

When evaluating NO_2 pollution on a per capita basis (expressed as 10^{15} Molecules cm^{-2} 10^6 Inhabitants^{-1}), a population-weighted metric for environmental quality, and subsequently

arranging the values in descending order [see Fig. 3(b)], it becomes evident that the most elevated levels are prevalent in UMICs as well. Megacities in HICs follow in the hierarchy (Chicago, Los Angeles, and Seoul). Notably, all megacities from LMICs are found at the lowermost part of the spectrum with the lowest per capita NO_2 pollution (Jakarta, Kolkata, Quezon City, Dhaka, Lagos, Ho Chi Minh City, Mumbai, Bengaluru, Delhi, Karachi, and Cairo) with the exception of Lahore, Pakistan, which deviates from this pattern and exhibits higher per capita pollution levels.

As we reveal that the per capita NO_2 pollution levels in LMICs are the lowest, this should be interpreted in the context of their increasing pollution trends, suggesting potential deterioration of air quality over time. Contrarily, although megacities from HICs show decreasing trends indicating improving air quality, the per capita pollution is still among the highest.

In general, we can identify two opposing developments: if the NO_2 trends of LMICs and HICs persist, with an increase and a decrease, respectively, the two groups will swap their positions in the hierarchy in the per-capita pollution [see bar chart Fig. 3(b)]. Finally, megacities from UMICs, displaying the highest positive relative NO_2 trends, also exhibit high per capita pollution levels. This dichotomy highlights the intricate relationship between economic development and environmental quality, underscoring the complex nature of their interactions.

In comparison to the trends of NO_2 pollution, settlement growth rates are only positive throughout the 38 megacities under analysis. Nevertheless, we also observe a high variability—from close to stagnation to extreme expansion. Fig. 4 presents the yearly growth of settlement area (expressed in km^2) for a selection of the megacities and the time period of 1996 to 2015.

For this period of 20 years in the megaregion Guangzhou (Pearl River Delta), China, the highest growth in built-up area is measured. There, an expansion by 3511 km^2 (approximately the area of the city/state of Berlin, Germany) is mapped, followed by Shanghai (2423 km^2) and Beijing (1790 km^2). In contrast, Lima and Karachi show only a small increase in built-up area of 46 km^2 and 134 km^2, respectively. Over the years, most megacities exhibit a straight linear increase of built-up areas. However, we also observe a pronounced flattening of the slope for Los Angeles in 2008, Chicago in 2006, and Wuhan in 2011, indicating a slowdown of the quantitative urbanization, i.e., expansion of built-up area that could be attributed to economic developments like the economic crisis in 2008 in the case of Los Angeles. On the contrary, Bangkok indicates a sharp increase in 2013 as well as Tokyo in 2014.

Based on the times series of the absolute settlement growth, the relative growth of the built-up area (%/year) was calculated for the time period from 1996 to 2015. Accordingly, in Fig. 5, the relative growth of settlement area (%/year) is presented for each megacity sorted by size. Here, Chengdu (see also Fig. 2), Chongqing, and Shanghai indicate the highest growth rates of 9.54%/year, 9.03%/year, and 7.70%/year, respectively. The lowest relative growth rates can be identified for Kinshasa (0.27%/year), Lima (0.38%/year), and Los Angeles (0.56%/year). The average relative settlement growth rate for all megacities is 2.87%/year and the median 1.85%/year.

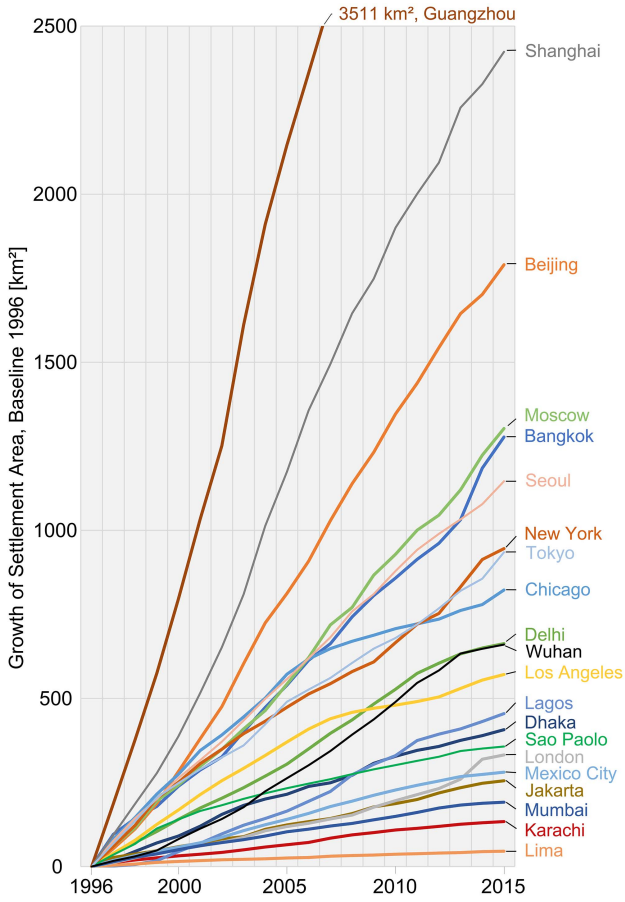

Fig. 4. Growth of settlement area in km^2 for a selection of megacities from 1996 to 2015 within their FUA. Note that 1996 is used as the baseline year.

Consistently with the analysis of the NO_2 trends, we put these findings in relation to the income groups following the world's economies classification of the World Bank. It can be observed that among the top ten megacities with the highest relative increase in built-up area, eight cities belong to UMICs. Actually, seven out of these ten megacities are located in China (Chengdu, Chongqing, Shanghai, Wuhan, Tianjin, Guangzhou, and Beijing). In contrast, the megacities with the lowest growth rates are attributed to the HICs. Further, it should be noted that megacities of LMICs predominantly appear in the center of the spectrum except for Bengaluru, India, and Ho Chi Minh City, Vietnam.

Megacities from the HICs are found among the smaller growth rates, with the exception of Seoul, South Korea (HIC), on rank 12 with relative growth rates of 3.36%/year, which stands for a very dynamic expansion for a megacity of an HIC. At the lowest end of the spectrum, we find Kinshasa (LIC) that is limited in growth by the Congo River and Lima (UMIC) that is strongly confined in growth by the ocean on the one hand and the Andes mountain range on the other hand (see also lower panel of Fig. 2). From Fig. 5, we can infer a dynamic cycle pertaining to urbanization and economic development levels. Megacities in LMICs display a moderate relative settlement growth, which, on average, intensifies during the transition to the UMIC class. In

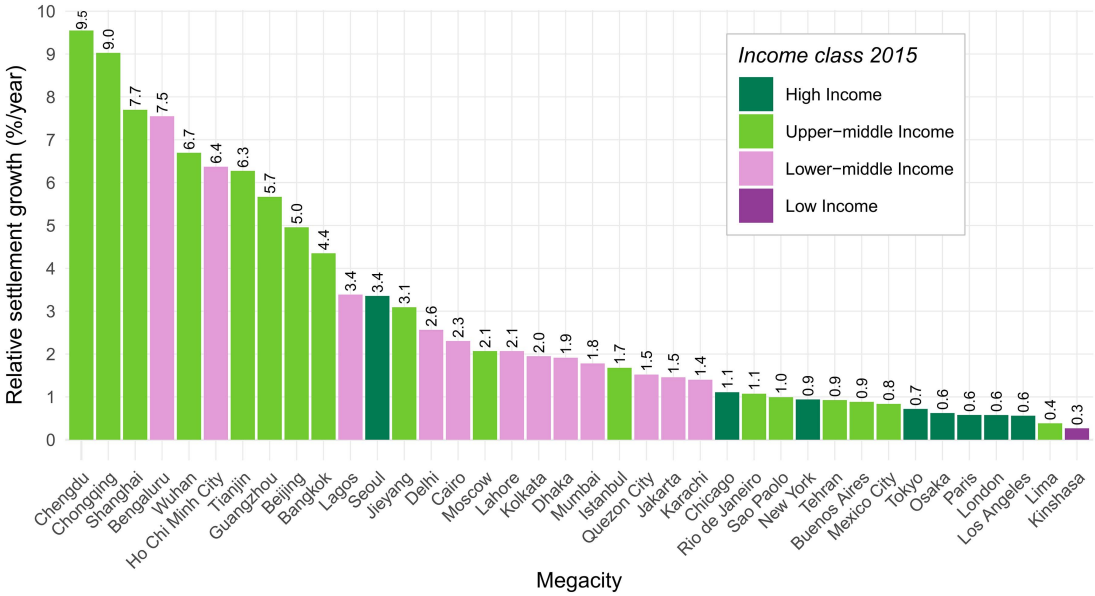

Fig. 5. Relative growth of the settlement area (%/year) for each of the 38 megacities and the time period 1996 to 2015 with respect to the FUAs. The income groups are overlaid following the world's economies classification of the World Bank [52].

the mature stages of HIC development, the relative settlement growth regresses to the lowest values, indicative of a state of saturation.

In Fig. 6, the results of the study are summarized by depicting the relative growth of settlement area (%/year) versus the relative NO_2 trend (%/year) for the 38 megacities under investigation. The error bars indicate the uncertainty of the NO_2 linear trend (5). The colors of the dots correspond to the income group classification of the World Bank, the size of the dots scales with the size of the FUA (km^2) according to GHSL_FUA. At a glance, we can see that megacities in HICs are concentrated in the lower left part exhibiting low relative settlement growth and predominantly negative relative tropospheric NO_2 trends (improving air quality). On the contrary on the upper right part of the plot, we find megacities of UMICs characterized by pronounced relative settlement growth and strong positive relative NO_2 trends. By means of the identity line (red dashed line), we can initially interpret the statistical relationship of the megacities concerning settlement and pollution development. While Bengaluru, Guangzhou, Bangkok, Quezon City, and all cities of HICs display a behavior with dynamic settlement growth and small increases or decreases in NO_2 pollution, Chongqing, Chengdu, Tianjin, Wuhan, Beijing, Dhaka, Lima, Tehran Lahore, and Karachi reveal a pronounced relation with disproportionately strong increases in NO_2 levels. Most strikingly Lima depicts a strong increase in air pollution while the settlement growth is the second weakest among the megacities. This can be explained by a strong internal concentration and agglomeration due to as said before limited expansion possibilities due to the coast and the Andes mountain range (see Fig. 2). Concerning FUA size, we observe that the megacities with the largest sizes can be found below the identity line. Only Moscow, Lagos, and Kinshasa are characterized by a proportional behavior (considering their levels of uncertainty).

To further examine the statistical relationship between the two quantities, we tested different regression models, such as linear, quadratic, and cubic polynomial models, and evaluated their performance by the statistical parameters R-squared (R^2), root-mean-squared error (RMSE), Akaike information criterion (AIC), and Bayesian information criterion (BIC). The linear regression is outperformed by both the quadratic regression and the cubic polynomial regression with $R^2 = 0.439 < 0.505 < 0.544$, respectively. In addition, the RMSE is the lowest with the cubic fit (RMSE $= 0.544$), followed by the quadratic fit (RMSE $= 6.177$) and the linear regression (RMSE $= 6.576$). Regarding AIC and BIC, lower values indicate a better tradeoff between goodness of fit and model complexity. The AIC is the smallest for the cubic polynomial fit. For the BIC, the values are very close and as such an interpretation is difficult: with 260.77, the quadratic regression exhibits the lowest value compared to 261.30 for the cubic regression and 261.90 for the linear regression. Following the evaluation of the different models, we have finally chosen the cubic polynomial regression to best explain the statistical relationship between relative NO2 trends and relative settlement growth. We find that it better captures the nonlinear relationship between the variables.

We test the null hypothesis that there is no statistical relationship between settlement growth and NO_2 trends. With a p-value $= 0.223$, we may accept the null hypothesis and suggest that there is no evidence in favor of a relationship between the two variables. Since statistical significance should be interpreted in the context of the specific analysis, we need to point out that the regression is strongly driven by a few cities with very high increases in settlement growth and NO_2 pollution from 1996 to 2015, namely, Chongqing, Chengdu, and Tianjin. Although they are no "outliers" in a statistical sense, their impact on the regression analysis asks for a careful interpretation of the findings.

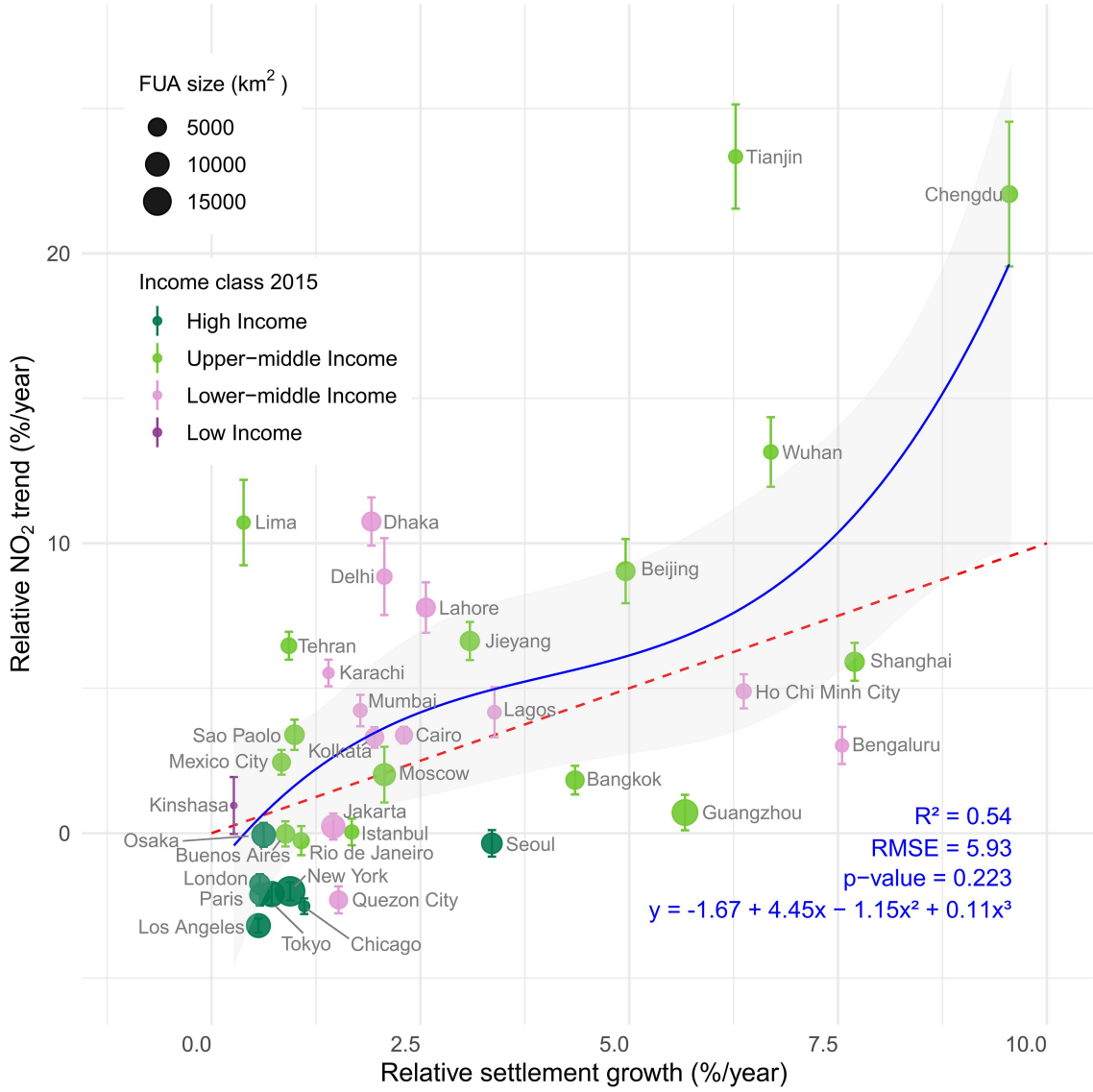

Fig. 6. Relative growth of settlement area versus relative tropospheric NO_2 trend for 38 megacities. The colors of the dots correspond to the income groups following the world's economies classification of the World Bank [52], and the size of the dots scales with the size of the FUA (km^2) according to GHSL_FUA [50]. The error bars indicate the uncertainty of the linear NO_2 trend. The dashed red line indicates the identity line, the blue line shows the regression, with its parameters, R^2 and p-value, in the lower right. Note that Chongqing at 9.5/44.0 is omitted in the plot, but not in the statistics.

Despite the observed variety among the megacities indicating different stages of, e.g., socioeconomic development or green transition, the megacities of the Global North are—as outlined before—clustered in the lower left characterized by decreasing pollution levels and small relative settlement growth rates (Los Angeles, New York, Chicago, London, and Paris). To derive a more diversified spectrum of megacity types, the grouping of megacities is further examined by k-means clustering using only the EO-derived parameters, including relative growth of settlement area (%/year), relative NO_2 trend (%/year), and mean tropospheric NO_2 column density (10^{15} Molecules/cm^2). The unsupervised classification distinguishes five classes (Fig. 7). Class 1 (red) comprises four large Asian megacities from HICs (Seoul) and UMICs (Beijing, Guangzhou, and Shanghai) with high tropospheric NO_2 pollution and dynamic settlement growth. Class 2 (ocher) encompasses seven cities of MICs with moderate to high relative NO_2 trends in the range of 6.5 ± 0.5%/year to 13.1 ± 1.2%/year (Wuhan, Dhaka, Lima, Lahore, Delhi, Jieyang, and Tehran). Class 3 (green) corresponds to the abovementioned megacities from HICs and the Global North—except for Seoul—clustered in the lower left with improving NO_2 air quality and small relative settlement growth (Los Angeles, Chicago, Paris, Tokyo, New York, London, and Osaka). However, we also find in class 3 megacities from UMICs, namely, Mexico City, Moscow, and Istanbul. Class 4 (light blue) embraces the largest group of megacities. They are characterized by low to moderate relative NO_2 trends and low to moderate NO_2 mean values. Kinshasa from an LIC is located here. Class 5 (magenta) consists of three cities with the strongest relative NO_2 increase and settlement growth that started in 1996 with low values and small urban

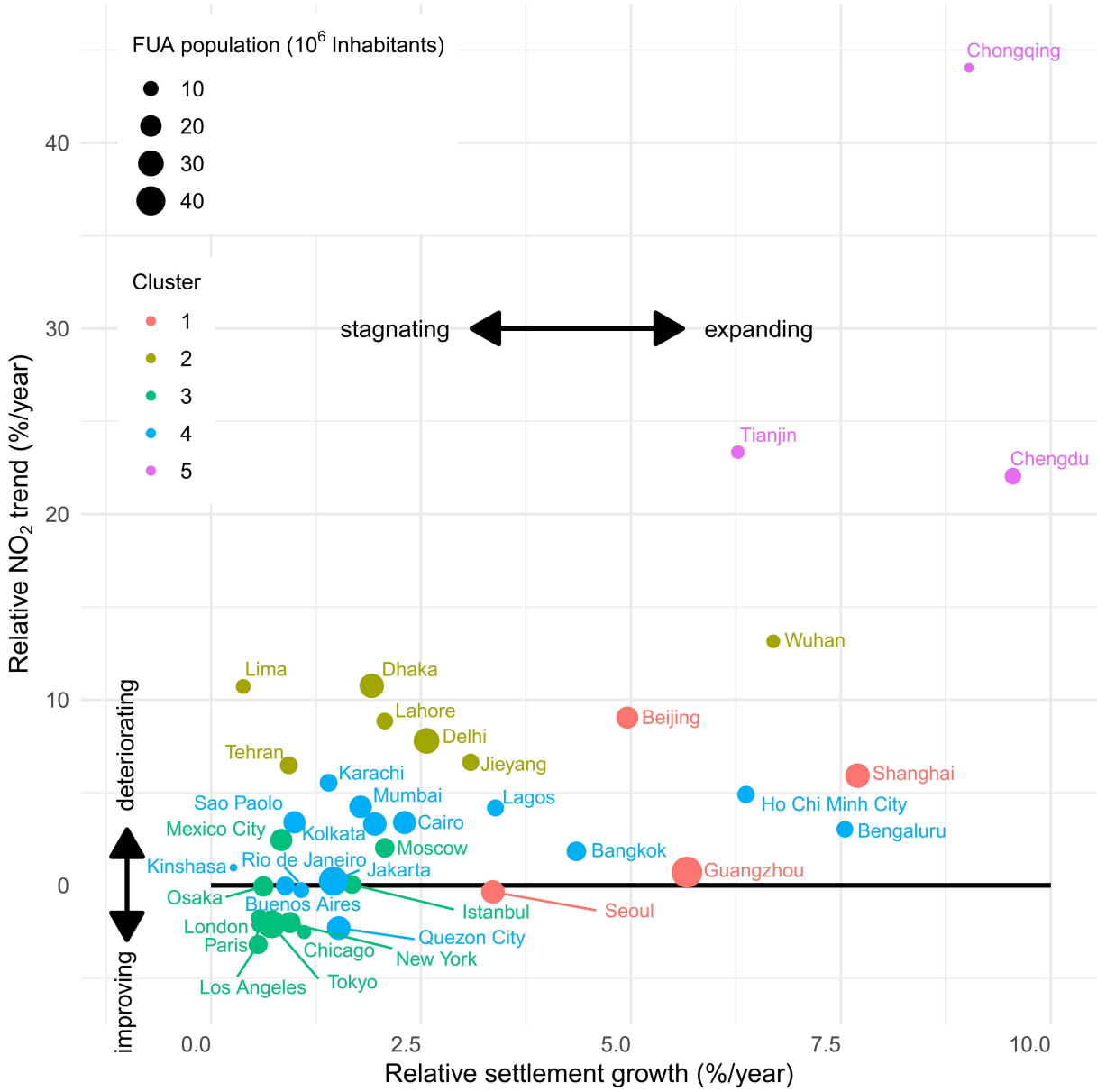

Fig. 7. Classification of megacities by k-means clustering. Five distinct groups were identified using the parameters relative growth of settlement area, relative NO_2 trend, and mean tropospheric NO_2 column density. The size of the dots scales with the FUA population (10^6 inhabitants).

area sizes. Finally, Fig. 7 allows for a straightforward and comprehensive classification of the development trajectories of the megacities under investigation. This classification extends to discerning whether these megacities are progressing towards improved environmental conditions, such as the green transition of the economy, or experiencing deterioration, as well as whether they are in a state of stagnation, concentration, or expansion concerning their settlement areas.

V. Discussion

In this article, aspects of NO_2 air pollution trends as well as settlement growth were systematically examined and compared for and across 38 megacities worldwide. Therefore, multiannual records of satellite-based tropospheric NO_2 observations and the evolution of the settlement footprint were exploited covering a period of 20 years. A special feature in this study is the use of the spatial concept of FUAs enabling consistent comparisons without distortions due to simplified, nontransparent, or heterogeneous reference units. Compared to most previous studies, the results advance beyond a pure presentation of NO_2 trends by systematically incorporating variables on urbanization, socioeconomy, and demography in the analysis.

A. Comparison of Results With Previous Studies

A critical discussion of the results obtained against the body of literature, i.e., published trends and settlement growth rates,

proves difficult due to missing or different spatial reference units and differing observation periods. To overcome parts of this challenge, we suggest the application of FUAs in this study. Due to the weak representativity of ground-based measurements for the large spatial extent of megacities, a comparison against our approach that integrates over the FUAs proves difficult, too. Furthermore, a satellite-based comparison of NO_2 trends and settlement growth does not yet exist to the best of the authors' knowledge. However, we can discuss in following the tendencies and identify agreements and differences. The direct reference regarding relative NO_2 trends is the work of Georgoulias et al. [40] that investigated several megacities and urban agglomerations. However, the time period differs (1996 to 2017) and no spatial definition for the derived trends is provided. Overall, the tendencies of the relative NO_2 trends agree. However, the highest positive trends observed in Chongqing (44%/year), Tianjin (23.3%/year), Chengdu (22.0%/year), and Wuhan (13.1%/year) exhibit a smaller amplitude in [40] with 28.1%/year, 14.9%/year, 11.7%/year, and 7.0%/year, respectively. This could be explained by the extreme dynamic settlement growth and expansion that has not yet been considered in [40] or the extended period, including 2017, since a beginning decrease of NO_2 was identified by the authors around 2012 due to the implementation of environmental measures and policies. Notably, a large deviation was found for Dhaka, where we report a relative NO_2 trend of 10.8%/year compared to 16.6% in the previous study. Due to the elongated urban shape of Dhaka, the different spatial references could be an explanation. The negative relative NO_2 trends can be confirmed for all megacities of HICs, with the exception of the Japanese megacities of Tokyo and Osaka, where we derived negative trends (improving air quality) compared to small positive trends in [40]. Interestingly, the exceptional behavior of Quezon City (Manila) for a megacity of LMICs with significant negative NO_2 trends of -2.3%/year is confirmed by the previous study (-2.2%/year). The regressing NO_2 levels in Tokyo and Los Angeles have also been identified by Bichler et al. [58] and linked to economic effects.

As for the NO_2 trends, it is also difficult to directly compare settlement growth rates among different studies. Again, the spatial reference unit and the time period considered play a dominant role and may distort the numbers. With respect to relative settlement growth, the authors in [10] and [59] identified, for the periods 1990 to 2000 and 2000 to 2010, Dhaka as the megacity with the highest growth rate followed by Delhi, Jakarta, and Mumbai (where we only consider cities that occur in both studies). In the current study, Dhaka can be found in the midfield with 1.9%/year increase, while Delhi exhibits a stronger growth (2.6%/year) and Mumbai and Jakarta a weaker one with 1.8%/year and 1.5%/year, respectively. In our study, Shanghai (7.7%/year) and Beijing (5.0%/year) report the highest settlement growth among the megacities considered, compared to significantly smaller rates in [59]. However, both studies agree on the smallest growth rates for Tokyo, Buenos Aires, Rio de Janeiro, Paris, London, and Los Angeles. Notably, regarding the African megacities, Taubenböck [59] reported a similar growth dynamic for Cairo and Kinshasa, while they strongly differ in this study with Kinshasa revealing the smallest growth of all megacities (0.3%/year) and Cairo 2.3%/year, which is close to the average of 2.87%/year.

B. Strengths and Limitations of NO_2 Observations

The study proves the potential of today's satellite-based observations for studying the variability of the tropospheric composition. After all, these are retrieved from space-borne instruments that have not been specifically designed for the observation of tropospheric air pollutants in the beginning, but stratospheric O_3 [16], [51]. However, even for the GOME-instrument [16] that started its operation in 1995 with its coarse native spatial resolution of 320×40 km^2, anthropogenic signals in tropospheric NO_2 column densities, such as the urban weekly cycle, could be identified [26]. This substantiates the sensitivity to the lower boundary layer. Apart from the coarse spatial resolution for urban environments, further limitations of the observations used in this study comprise 1) the low temporal resolution of mainly one (morning) overpass per day due to a sun-synchronous near-polar low Earth orbit, 2) the dependence on solar-backscattered radiation, and 3) the cloud coverage that often persists in particular during pollution episodes, e.g., as a consequence of inversion conditions in the lower boundary layer. Of course, this means that daily variations or local intraurban hotspots cannot be monitored.

However, these satellite-based observations enable the quantification of global tropospheric NO_2 pollution and its trends as was substantiated already by other authors, e.g., see [31], [36], and [39]. By design, one operating space-borne instrument can be considered as a global transfer standard delivering consistent and homogeneous measurements worldwide. It must be borne in mind, however, that tropospheric NO_2 column densities are observed, i.e., retrieved and not the NO_2 mass concentration near the ground (in ambient air) as in-situ sensors do. With these data, however, all regions and cities can be systematically examined in an area-wide, consistent way, appropriate for multitemporal and across-space comparisons [40]. Such comprehensive, spatially integrating, multitemporal datasets are an important data asset to complement ground-based measurements, as their limited spatial representativeness and often scarce availability lead to uncertainties in the interpretation.

C. Uncertainty of NO_2 Observations

An important aspect of the trend analysis is the accuracy of the tropospheric NO_2 dataset. Following [60], the Level 2 processing chain enables to provide a realistic error budget for tropospheric NO_2 vertical column densities. The average uncertainty due to the tropospheric air mass factor over Europe is quantified by 18%–26% per pixel [61]. Other studies distinguish between uncertainties under polluted and unpolluted conditions [19], where the estimated uncertainty in the GOME-2 tropospheric NO_2 column for polluted conditions ranges from 40%–80% for a single observation. However, a detailed error analysis for individual retrievals exhibits a strong variation of these estimates [60]. The total error budget comprises contributions of the geophysical parameters cloud fraction, cloud pressure, surface albedo, surface pressure, the a priori NO_2 profile shape, and NOx

emissions as well as aerosol-related errors. Following [19], the most important uncertainties associated with the computation of the tropospheric air mass factor are cloud fraction, surface albedo, and the a priori NO_2 profile. Over polluted regions, air-mass factor errors contribute substantially to the overall error. The overall error of the tropospheric NO_2 columns is driven by error propagation of the error terms listed before. Since a monthly mean dataset is built from daily observations (with sample size n) [40] and the standard error decreases by $1/\sqrt{n}$, the overall error can be strongly reduced. For a campaign in Europe, monthly mean tropospheric columns are in very good agreement, with differences generally within 0.5×10^{15} molecules cm^{-2} [19]. However, with respect to the systematic error, a comparison of tropospheric NO_2 column densities to global ground-based measurements shows, on average, a negative bias of typically $-23\,\%$ to $-37\,\%$ in clean to slightly polluted conditions, but reaching values as high as $-51\,\%$ over highly polluted areas [62]. A part of the biases can be explained by differences in the representativity of the stations and different area averaging and measurement times. It is also known that errors in the tropospheric columns result from shortcomings in the horizontally coarse a priori profile representation in the underlying chemical transport model used in the retrieval [20]. Therefore, the tropospheric NO_2 retrieval could be significantly improved by using a priori profiles from a CTM with much higher spatial resolution and a more realistic cloud treatment [63].

In spite of the occurrence of NO_2 transport between urban areas and the surrounding regions, the relatively short atmospheric lifetime of NO_2, ranging from a few hours to a day, ensures that its concentrations predominantly reflect the local strength of NO_2 emissions [15], [20]. Despite the limitations, satellite data of the last decades have already been used to analyze the background pollution and the trend development around the world [31], [36], [39].

D. Strengths and Limitations of the WSF

The WSF has proven to be an effective geo dataset for large-scale mapping of human settlements at $30 \times 30\,m^2$ spatial resolution on a global scale [10], [44], [45]. With the WSF evolution available on a yearly basis, this study quantifies and analyses the horizontal expansion of megacities. We believe that this is a valid and consistent systematic approach to study this aspect of urbanization and megacity evolution. However, although the mapping product has achieved high accuracies, spatially uneven distributed classification errors have been documented [44], [46].

In addition, it is known that in certain development cycles, a vertical growth in cities cannot be neglected. In particular, this occurs with the development and strengthening of (central) business districts or large-scale housing developments with high-rise or mid-rise buildings for living. However, multitemporal settlement data, including the evolution in the third dimension with sufficient accuracy, are still absent. Latest developments, however, show that these mapping products will become more and more available [47], [64], [65], [66].

The WSF is a binary classification of "settlement" and "non-settlement." It is clear that urban areas and especially large urban regions, such as megacities, exhibit intraurban structural and functional variations [67]. This is also associated with different sources of NO_2 emissions. Thematically, higher resolution classifications of urban structural configurations of urban landscapes are emerging [68], but are not available multitemporally for the monitoring period. This intra-urban differentiation, however, may provide new insights as a research topic in the future.

E. Multicity Studies and Spatial Consistent Concepts

Many studies concentrate on a single or a limited number of selected cities, thereby raising concerns regarding the generalizability of conclusions and the applicability of findings to other urban or regional contexts, e.g., [58]. The need for multicity studies was recently raised [69]. The current study contributes to serving this demand since it provides a systematic analysis of all megacities worldwide and empowers to derive general conclusions.

The demand for multicity studies also raises the need for appropriate and geographically consistent reference units [42]. However, geographically inconsistent spatial city extents, such as administrative areas, remain the key reference units in most studies. Therefore, it is often difficult to perform a solid comparison without distorted statistics, to draw general conclusions, or to compare results across scientific contributions. The inconsistencies of population numbers are obvious in Table I when comparing numbers from the UN [8] versus the GHSL-FUA [50] resulting from different statistical approaches and underlying spatial concepts. Contrary to previous studies on tropospheric NO_2 trends, this work advances on the approach by a systematic analysis of megacities worldwide considering pollution in combination with settlement growth and the spatial concept of FUAs providing comparable geographic units. To the best of the authors' knowledge, this consistent analysis is currently not available. Furthermore, a thorough investigation of this 20-year period by means of a consistent spatial concept lays also down the fundament for follow-up studies. On the one hand, the analysis that was carried out for the FUAs of the epoch 2015 could be expanded toward their multitemporal development. On the other hand, different data-driven approaches for consistently delineating megacities, such as the degree of urbanization [70], morphological urban areas [42], or spatially continuous ways of measuring the urban and the nonurban [71], could be applied, and the stability of the results tested.

F. Dependence of Results on Time Period Considered

One might argue that the time period considered in the study is outdated and that the latest developments of air pollution levels as a consequence of implementing measures and actions are not considered, such as the policies to reduce air pollution in China or India starting around 2010. First of all, the study is based on the newest and most consistent datasets available. Second, it establishes the period from 1996 to 2015 as the baseline of the study, which results from the overlapping period of the WSF evolution (1985 to 2015) on the one hand and the beginning of

tropospheric composition mapping in 1995/1996 with GOME and successors to present on the other hand. Third, evaluating past air pollutant trends in urban areas gives insight into the effectiveness of previous or recently implemented policies [29]. The results attained here can serve as the baseline to examine the effectiveness of current policies to control air pollution and urban sprawl, and possibly support measures for future policies [13]. The policy in China for example has reversed the NO_2 trends partly from a strong increase into a decrease in the meantime, thanks to the implementation of mitigation measures, i.e., NO_x emission reductions. This reversal cannot be appropriately acknowledged by neglecting the situation in the decades before. A thorough evaluation of trends is a prerequisite for studying the effects of policy implementations like the introduction of emission taxes on pollution levels and economic value [72]. In general, however, the study will be performed from 2016 to the present as soon as the update of the WSF evolution will be available. This will provide a better statistical basis to identify trend reversals as initiated in [40].

G. Megacity Development and Global Economic Landscape

As early as in 1992, Shukla and Parikh [73] addressed the need for an empirical examination of differences and similarities between cities from the Global North and the Global South concerning air pollution, urbanization, and city size. At that time, based quite on speculative terms, cities from less developed countries were thought to hold more potential for much greater pollution than it was anticipated for developed economies. This assumption was based on the fact that they had to go a long path of industrialization and had more limited means to mitigate environmentally detrimental concomitants of this process. Therefore, Shukla and Parikh [73] made an initial step toward assessing the magnitude of one aspect of the problem that cities from developing countries are facing, air pollution. In doing so, they conducted an empirical examination of differences and similarities between the two contexts. Cities of the Global South are characterized by greater population pressures, more rapid urbanization rates, the unbalanced growth of megacities beyond limits, and the elevated use of resources predicated by more appropriate technologies to higher development levels [8]. As presented in the current work, we can demonstrate what EO has accomplished in the meantime, by providing global datasets for comprehensive documentation and studies. As we neither use the concept of developed and developing countries nor Global North and Global South, we apply the global income classification of the World Bank that gives a much more detailed view. Furthermore, different groups are in a different stage of the economic development and as such in different technological and socioeconomic cycles.

Given the EO data records covering 20 years, we can take the opportunity to revisit development trends. In particular, by analyzing EO data records that have now become available, we retrospectively contribute to answering the hypothesis whether the sizes of megacities are dynamically growing in less developed countries and whether the growth rate in major metropolitan areas in more developed countries is declining. In general, we confirm the hypothesis, but the systematic analysis of all megacities allows us to identify exceptions. As was shown in this study, Seoul is measured with exceptionally high settlement growth rates for a city in an HIC. On the contrary, Kinshasa and Lima show the lowest relative settlement growth rates although the cities are from LICs and MICs. Despite the low settlement growth rate in the time period considered, Kinshasa is predicted by the UN to become home to 58.42 million people by 2075. Furthermore, Chicago is supposed to become the fastest developing megacity from the HICs. Other emerging megacities are Dar es Salaam, Luanda, Baghdad, Chennai, and Bogota. The continuous monitoring of the tropospheric composition and the settlement footprint will be inevitable to track the development, urbanization, and environmental impact of existing and emerging megacities worldwide.

When analyzing relative settlement growth rates and interpreting them within the global economic landscape, we need to keep their relation to the size of the FUAs under consideration in mind. Due to the large size of the FUA of Los Angeles (10 407 km^2) for example and its built-up area in 1996 of 5091 km^2, a relative increase in settlement area of 0.6%/year corresponds to an increment of built-up area in 2015 by 571 km^2. This exceeds the increase in the settlement area of, e.g., Lagos that exhibits a higher relative growth of 3.4%/year corresponding to an increase in built-up area of 455 km^2. However, for reasons of comparison, we justify the concept of relative numbers, since it is a measure of the progress of settlement growth and its impact on the megacity.

H. Transformative Aspects

Social, economic, and environmental justice and substantiating findings on air inequality are in demand. The study so far neglects transformative aspects since it currently does not consider social or socioeconomic aspects in detail. This has not yet been included in the current work for the following reasons: these aspects cannot (yet) be derived directly from or tackled with EO data. As such, the data available for megacities are derived by varying methods and are not available in a complete or consistent manner for the FUAs across the globe. The social or socioeconomic data currently available are provided for different administrative units, often only on aggregated scales such as national levels thus resulting in global data heterogeneity and uncertainty which hinders reliable conclusions. Also, the statistics of the World Bank applied in this study are based on national aggregates and should be interpreted carefully to capture or disentangle developments of an individual city. However, the significance of megacities in a country and their large share to most socioeconomic and environmental factors justify the assumptions made in this work.

I. Perspectives on Integrated Air Pollution Assessments

However, in order to consider the total air pollution situation in the megacities and to assess the associated health risks, the integration of other air pollutants, such as fine particular matter and O_3, are in demand. Therefore, the comparison of megacities, as presented here, needs to be interpreted carefully. We do refer

to tropospheric NO_2 only. While the distributions and trends of NO_2 predominantly reflect anthropogenic emission behavior, variability and changes in meteorological parameters may also play a decisive role. However, the time series analysis method used in this article should result in robust estimates and cope with seasonal and annual fluctuations [34]. Air pollution levels and the resulting (long-term) trends may also be subject to influences from other parameters and processes, such as changes in precipitation, the number of fog days or the concentration, and type of aerosols. Ultimately, more detailed and systematic studies are needed to investigate possible changes in the chemical regime of the megacities.

Current satellite missions and instruments, such as Sentinel-5P/TROPOMI and GEMS, and the upcoming missions (Sentinel-4, Sentinel-5, and TEMPO) will provide unprecedented opportunities for studying the tropospheric chemical composition. In particular, by combining LEO and GEO orbits, which will resolve diurnal cycles of the atmospheric composition, we will be able to much better observe and analyze air pollution variability in megacities and megaregions worldwide.

VI. Conclusion

A first systematic analysis of megacities in relation to tropospheric NO_2 pollution trends and settlement area growth was presented. The results advance beyond a pure presentation of NO_2 trends by systematically incorporating variables on urbanization, socioeconomy, and demography in the analysis. The study covers a period of 20 years (1996 to 2015). By consistently applying the spatial concept of FUAs, we find that the megacities on average exhibit an increase in tropospheric NO_2 burden of $5.06 \pm 0.83\%$/year. The average relative settlement growth rate for the megacities is 2.87%/year. Among the 38 megacities under investigation, a wide range from increasing to decreasing NO_2 pollution levels was derived and, with respect to settlement area growth, cities with stagnating to highly dynamic growth rates. In terms of absolute growth of the built-up area, we report increases from 16 km^2 (Kinshasa, Democratic Republic of the Congo) and 46 km^2 (Lima, Peru) to 3511 km^2 (Guangzhou, China). Despite the variety, we found that the results exhibit a pronounced relation to the income groups following the world's economies classification of the World Bank. While the strongest increase of NO_2 pollution and settlement growth as well as per-capita pollution occur in megacities of UMICs, megacities of LMICs are centered in the midfield of the spectrum, but with the lowest per-capita pollution levels. Megacities in HICs are predominantly characterized by the smallest relative settlement growth rates and a decrease in NO_2 air pollution. Conversely, despite the decreasing trends observed in megacities from HICs, indicating advancements in air quality, the per capita pollution levels in these cities persist at some of the highest levels. This dichotomy underscores the complex interplay between economic development, urbanization, and environmental quality.

We conclude that the combination of tropospheric NO_2 composition records and the WSF evolution provide essential components to develop a better understanding of the drivers and impacts of urbanization and air pollution. Regression analysis indicated a statistical relationship between relative settlement growth and relative NO_2 increase among the megacities.

Furthermore, we conclude that the presented approach is suitable for identifying and comparing megacities concerning their socioeconomic development and transformation stages, such as the green transition and world economies. By a simple classification of EO-based parameters, we can label the megacities in their transformation stage. We can infer a dynamic cycle pertaining to urbanization and economic development levels.

Finally, we conclude that the findings give insight into the effectiveness of previous and current urban policies and developments, and possibly support future measures to transform existing cities according to the United Nations Sustainable Development Goal SDG 11 ("Make Cities Inclusive, Safe, Resilient and Sustainable").

Acknowledgment

The authors would like to thank Tropospheric Emission Monitoring Internet Service (https://www.temis.nl/) for the free use of tropospheric NO_2 data.

References

[1] World Health Organization, "WHO global air quality guidelines: Particulate matter (PM2.5 and PM10), ozone, nitrogen dioxide, sulfur dioxide and carbon monoxide," World Health Organization, Geneva, Switzerland, 2021. [Online]. Available: https://www.who.int/publications/i/item/9789240034228

[2] I. Manisalidis, E. Stavropoulou, A. Stavropoulos, and E. Bezirtzoglou, "Environmental and health impacts of air pollution: A review," *Front. Public Health*, vol. 8, 2020, Art. no. 505570, doi: 10.3389/fpubh.2020.00014.

[3] L. Gilardi, M. Marconcini, A. Metz-Marconcini, T. Esch, and T. Erbertseder, "Long-term exposure and health risk assessment from air pollution: Impact of regional scale mobility," *Int. J. Health Geograph.*, vol. 22, no. 1, 2023, Art. no. 11, doi: 10.1186/s12942-023-00333-8.

[4] J. Rittweger et al., "Temperature and particulate matter as environmental factors associated with seasonality of influenza incidence – an approach using Earth observation-based modeling in a health insurance cohort study from Baden-Württemberg (Germany)," *Environ. Health*, vol. 21, 2022, Art. no. 131, doi: 10.1186/s12940-022-00927-y.

[5] D. Weismann, M. Möckel, H. Paeth, and A. Slagman, "Modelling variations of emergency attendances using data on community mobility, climate, and air pollution," *Sci. Rep.*, vol. 13, Art. no. 20595, 2023, doi: 10.1038/s41598-023-47857-4.

[6] J. Lelieveld, A. Pozzer, U. Pöschl, M. Fnais, A. Haines, and T. Münzel, "Loss of life expectancy from air pollution compared to other risk factors: A worldwide perspective," *Cardiovasc. Res.*, vol. 116, pp. 1910–1917, 2020, doi: 10.1093/cvr/cvaa025.

[7] World Bank, "Urban development overview," 2022. [Online]. Available: https://www.worldbank.org/en/topic/urbandevelopment/overview

[8] United Nations, "World urbanization prospects 2018," Department of Economic and Social Affairs – Population Dynamics, 2018. [Online]. Available: https://population.un.org/wup/

[9] M. J. Molina and L. T. Molina, "Critical review: Megacities and atmospheric pollution," *J. Air Waste Manage. Assoc.*, vol. 54, no. 6, pp. 644–680, 2004, doi: 10.1080/10473289.2004.10470936.

[10] H. Taubenböck, T. Esch, A. Felbier, M. Wiesner, A. Roth, and S. Dech, "Monitoring urbanization in mega cities from space," *Remote Sens. Environ.*, vol. 117, pp. 162–176, 2012, doi: 10.1016/j.rse.2011.09.015.

[11] P. Huszar, J. Karlický, J. Marková, T. Nováková, M. Liaskoni, and L. Bartík, "The regional impact of urban emissions on air quality in Europe: The role of the urban canopy effects," *Atmospheric Chem. Phys.*, vol. 21, pp. 14309–14332, 2021, doi: 10.5194/acp-21-14309-2021.

[12] C. He et al., "Air pollution interactions with weather and climate extremes: Current knowledge, gaps, and future directions," *Curr. Pollut. Rep.*, 2024, doi: 10.1007/s40726-024-00296-9.

[13] A. Baklanov, L. T. Molina, and M. Gauss, "Megacities, air quality and climate," *Atmospheric Environ.*, vol. 126, pp. 235–249, 2016, doi: 10.1016/j.atmosenv.2015.11.059.

[14] B. N. Duncan et al., "The observed response of Ozone monitoring instrument (OMI) NO_2 columns to NO_x emission controls on power plants in the United States: 2005–2011," *Atmospheric Environ.*, vol. 81, pp. 102–111, 2013, doi: 10.1016/j.atmosenv.2013.08.068.

[15] K. Lange, A. Richter, and J. P. Burrows, "Variability of nitrogen oxide emission fluxes and lifetimes estimated from Sentinel-5P TROPOMI observations," *Atmospheric Chem. Phys.*, vol. 22, pp. 2745–2767, 2022, doi: 10.5194/acp-22-2745-2022.

[16] J. P. Burrows et al., "The global ozone monitoring experiment (GOME): Mission concept and first scientific results," *J. Atmospheric Sci.*, vol. 56, pp. 151–175, 1999, doi: 10.1175/1520-0469(1999)056%3C0151:TGOMEG%3E2.0.CO;2.

[17] T. Erbertseder, H. Taubenböck, and J. Meyer-Arnek, "Stadtregionen als globale Zentren der Luftverschmutzung," in *Globale Urbanisierung -Perspektive aus Dem All*, H. Taubenböck, M. Wurm, T. Esch, and S. Dech, Eds., Berlin, Germany: Springer, 2015, pp. 191–203, doi: 10.1007/978-3-662-44841-0_20.

[18] A. Richter and J. P. Burrows, "Tropospheric NO_2 from GOME measurements," *Adv. Space Res.*, vol. 29, no. 11, pp. 1673–1683, 2002.

[19] P. Valks et al., "Operational total and tropospheric NO_2 column retrieval for GOME-2," *Atmospheric Meas. Techn.*, vol. 4, pp. 1491–1514, 2011, doi: 10.5194/amt-4-1491-2011.

[20] I. Müller, T. Erbertseder, and H. Taubenböck, "Tropospheric NO_2: Explorative analyses of spatial variability and impact factors," *Remote Sens. Environ.*, vol. 270, 2022, Art. no. 112839, doi: 10.1016/j.rse.2021.112839.

[21] T. Erbertseder, F. Baier, and C. Bergemann, "Der Wochenrhythmus der Städte – Erfassung anthropogener Aktivitätsmuster aus dem All," in *Globale Urbanisierung – Perspektive Aus Dem All*, H. Taubenböck, M. Wurm, T. Esch, and S. Dech, Eds., Berlin, Germany: Springer, 2015, pp. 151–158, doi: 10.1007/978-3-662-44841-0_16.

[22] C. Voigt et al., "Cleaner skies during the COVID-19 lockdown," *Bull. Amer. Meteorological Soc.*, vol. 103, no. 8, pp. E1796–E1827, 2022, doi: 10.1175/BAMS-D-21-0012.1.

[23] F. J. Pérez-Invernón et al., "Quantification of lightning-produced NOx over the Pyrenees and the Ebro Valley by using different TROPOMI-NO_2 and cloud research products," *Atmospheric Meas. Techn.*, vol. 15, no. 11, pp. 3329–3351, 2022, doi: 10.5194/amt-15-3329-2022.

[24] X. Lu et al., "The underappreciated role of agricultural soil nitrogen oxide emissions in ozone pollution regulation in North China," *Nature Commun.*, vol. 12, 2021, Art. no. 5021, doi: 10.1038/s41467-021-25147-9.

[25] A. Samad et al., "Meteorological and air quality measurements in a city region with complex terrain: Influence of meteorological phenomena on urban climate," *Meteorologische Zeitschrift*, vol. 32, no. 4, pp. 293–315, 2023, doi: 10.1127/metz/2023/1124.

[26] S. Beirle, U. Platt, M. Wenig, and T. Wagner, "Weekly cycle of NO_2 by GOME measurements: A signature of anthropogenic sources," *Atmospheric Chem. Phys.*, vol. 3, pp. 2225–2232, 2003, doi: 10.5194/acp-3-2225-2003.

[27] T. Stavrakou, J. F. Müller, M. Bauwens, K. F. Boersma, and J. van Geffen, "Satellite evidence for changes in the NO_2 weekly cycle over large cities," *Sci. Rep.*, vol. 10, 2020, Art. no. 10066, doi: 10.1038/s41598-020-66891-0.

[28] R. F. Silvern et al., "Using satellite observations of tropospheric NO_2 columns to infer long-term trends in US NOx emissions: The importance of accounting for the free tropospheric NO_2 background," *Atmospheric Chem. Phys.*, vol. 19, pp. 8863–8878, 2019, doi: 10.5194/acp-19-8863-2019.

[29] D. L. Goldberg et al., "Urban NO_x emissions around the world declined faster than anticipated between 2005 and 2019," *Environ. Res. Lett.*, vol. 16, 2021, Art. no. 115004, doi: 10.1088/1748-9326/ac2c34.

[30] J. Ding, R. van der A, B. Mijling, J. de Laat, H. Eskes, and K. F. Boersma, "NO_x emissions in India derived from OMI satellite observations," *Atmospheric Environ. X*, vol. 14, 2022, Art. no. 100174, doi: 10.1016/j.aeaoa.2022.100174.

[31] A. Richter, J. P. Burrows, H. Nüß, C. Granier, and U. Niemeier, "Increase in tropospheric nitrogen dioxide over China observed from space," *Nature*, vol. 437, pp. 129–132, 2005, doi: 10.1038/nature04092.

[32] H. Bovensmann, J. P. Burrows, and M. Buchwitz, "SCIAMACHY - Mission objectives and measurement modes," *J. Atmospheric Sci.*, vol. 56, pp. 127–150, 1999.

[33] R. J. van der A et al., "Trends, seasonal variability and dominant NO_x source derived from a ten-year record of NO_2 measured from space," *J. Geophysical Res.: Atmos.*, vol. 113, 2008, Art. no. D04302, doi: 10.1029/2007JD009021.

[34] E. C. Weatherhead et al., "Factors affecting the detection of trends: Statistical considerations and applications to environmental data," *J. Geophysical Res.: Atmos.*, vol. 103, pp. 17149–17161, 1998, doi: 10.1029/98JD00995.

[35] P. Schneider and R. van der A, "A global single-sensor analysis of 2002-2011 tropospheric nitrogen dioxide trends observed from space," *J. Geophysical Res.: Atmos.*, vol. 117, no. D16, 2012, Art. no. D16309, doi: 10.1029/2012JD017571.

[36] P. Schneider, W. A. Lahoz, and R. van der A, "Recent satellite-based trends of tropospheric nitrogen dioxide over large urban agglomerations worldwide," *Atmospheric Chem. Phys.*, vol. 15, pp. 1205–1220, 2015, doi: 10.5194/acp-15-1205-2015.

[37] I. B. Konovalov, M. Beekmann, A. Richter, J. P. Burrows, and A. Hilboll, "Multi-annual changes of NOx emissions in megacity regions: Nonlinear trend analysis of satellite measurement-based estimates," *Atmospheric Chem. Phys.*, vol. 10, pp. 8481–8498, 2010, doi: 10.5194/acp-10-8481-2010.

[38] J. A. Geddes, R. V. Martin, B. L. Boys, and A. van Donkelaar, "Long-term trends worldwide in ambient NO_2 concentrations inferred from satellite observations," *Environ. Health Perspectives*, vol. 124, no. 3, pp. 281–289, Mar. 2016, doi: 10.1289/ehp.1409567.

[39] A. Hilboll, A. Richter, and J. P. Burrows, "Long-term changes of tropospheric NO_2 over megacities derived from multiple satellite instruments," *Atmospheric Chem. Phys.*, vol. 13, pp. 4145–4169, 2013, doi: 10.5194/acp-13-4145-2013.

[40] A. K. Georgoulias, R. J. van der A, P. Stammes, K. F. Boersma, and H. J. Eskes, "Trends and trend reversal detection in 2 decades of tropospheric NO_2 satellite observations," *Atmospheric Chem. Phys.*, vol. 19, pp. 6269–6294, 2019, doi: 10.5194/acp-19-6269-2019.

[41] A. Moreno-Monroy, M. Schiavina, and P. Veneri, "Metropolitan areas in the world. Delineation and population trends," *J. Urban Econ.*, vol. 125, 2021, Art. no. 103242, doi: 10.1016/j.jue.2020.103242.

[42] H. Taubenböck et al., "A new ranking of the world's largest cities—Do administrative units obscure morphological realities?," *Remote Sens. Environ.*, vol. 232, 2019, Art. no. 111353, doi: 10.1016/j.rse.2019.111353.

[43] H. Taubenböck et al., "New dimensions of urban landscapes: The spatio-temporal evolution from a polynuclei area to a mega-region based on remote sensing data," *Appl. Geography*, vol. 47, pp. 137–153, 2014, doi: 10.1016/j.apgeog.2013.12.002.

[44] M. Marconcini et al., "Outlining where humans live, the world settlement footprint 2015," *Sci. Data*, vol. 7, 2020, Art. no. 242, doi: 10.1038/s41597-020-00580-5.

[45] T. Esch et al., "Breaking new ground in mapping human settlements from space – The global urban footprint," *ISPRS J. Photogrammetry Remote Sens.*, vol. 134, pp. 30–42, 2017, doi: 10.1016/j.isprsjprs.2017.10.012.

[46] M. Marconcini, A. Metz-Marconcini, T. Esch, and N. Gorelick, "Understanding current trends in global urbanisation – The world settlement footprint suite," in *Proc. GI_Forum*, 2021, pp. 33–38, doi: 10.1553/giscience2021_01_s33.

[47] T. Esch et al., "World settlement footprint 3D - A first three-dimensional survey of the global building stock," *Remote Sens. Environ.*, vol. 270, 2022, Art. no. 112877, doi: 10.1016/j.rse.2021.112877.

[48] T. Erbertseder et al., "Earth observation-based analysis of NO_2 pollution and settlement growth in megacities," in *Proc. Joint Urban Remote Sens. Event*, 2023, pp. 1–4, doi: 10.1109/JURSE57346.2023.10144190.

[49] World Bank, "World Bank group country classifications by income level for FY24," 2023. [Online]. Available: https://blogs.worldbank.org/opendata/new-world-bank-group-country-classifications-income-level-fy24#_ftn1

[50] M. Schiavina, A. Moreno-Monroy, L. Maffenini, and P. Veneri, "GHS-FUA R2019A - GHS functional urban areas, derived from GHS-UCDB R2019A," European Commission, Joint Research Centre, 2020. [Online]. Available: https://data.jrc.ec.europa.eu/dataset/347f0337-f2da-4592-87b3-e25975ec2c95

[51] R. Munro et al., "The GOME-2 instrument on the metop series of satellites: Instrument design, calibration, and level 1 data processing – An overview," *Atmospheric Meas. Techn.*, vol. 9, pp. 1279–1301, 2016, doi: 10.5194/amt-9-1279-2016.

[52] World Bank, "New World Bank country classifications by income level: 2022-2023," 2022. [Online]. Available: https://blogs.worldbank.org/opendata/new-world-bank-country-classifications-income-level-2022-2023

[53] A. Wendleder, A. Schmitt, T. Erbertseder, P. D'Angelo, C. Mayer, and M. Braun, "Seasonal evolution of supraglacial lakes on Baltoro Glacier from 2016 to 2020," *Front. Earth Sci.*, vol. 9, 2021, Art. no. 725394, doi: 10.3389/feart.2021.725394.

[54] G. C. Tiao et al., "Effects of autocorrelation and temporal sampling schemes on estimates of trend and spatial correlation," *J. Geophysical Res.: Atmos.*, vol. 95, no. D12, pp. 20507–20517, 1990, doi: 10.1029/JD095iD12p20507.

[55] B. D. Santer et al., "Statistical significance of trends and trend differences in layer-average atmospheric temperature time series," *J. Geophysical Res.: Atmos.*, vol. 105, no. D6, pp. 7337–7356, 2000, doi: 10.1029/1999JD901105.

[56] S. Lloyd, "Least squares quantization in PCM," *IEEE Trans. Inf. Theory*, vol. 28, no. 2, pp. 129–137, Mar. 1982, doi: 10.1109/TIT.1982.1056489.

[57] R. L. Thorndike, "Who belongs in the family?," *Psychometrika*, vol. 18, pp. 267–276, 1953, doi: 10.1007/BF02289263.

[58] R. Bichler, S. S. Schönebeck, and M. Bittner, "Observing decoupling processes of NO_2 pollution and GDP growth based on satellite observations for Los Angeles and Tokyo," *Atmospheric Environ.*, vol. 310, 2023, Art. no. 119968, doi: 10.1016/j.atmosenv.2023.119968.

[59] H. Taubenböck, "Ohne limit? Die expansion von megacities," in *Globale Urbanisierung*, H. Taubenböck, M. Wurm, T. Esch, and S. Dech, Eds., Berlin, Germany: Springer, 2015, doi: 10.1007/978-3-662-44841-0_7.

[60] K. F. Boersma, H. J. Eskes, and E. J. Brinksma, "Error analysis for tropospheric NO_2 retrieval from space," *J. Geophysical Res.: Atmos.*, vol. 109, 2004, Art. no. D04311, doi: 10.1029/2003JD003962.

[61] K. F. Boersma et al., "Improving algorithms and uncertainty estimates for satellite NO_2 retrievals: Results from the quality assurance for the essential climate variables (QA4ECV) project," *Atmospheric Meas. Techn.*, vol. 11, pp. 6651–6678, 2018, doi: 10.5194/amt-11-6651-2018.

[62] T. Verhoelst et al., "Ground-based validation of the Copernicus sentinel-5P TROPOMI NO_2 measurements with the NDACC ZSL-DOAS, MAX-DOAS and Pandonia global networks," *Atmospheric Meas. Techn.*, vol. 14, pp. 481–510, 2021, doi: 10.5194/amt-14-481-2021.

[63] S. Liu et al., "An improved tropospheric NO_2 column retrieval algorithm for TROPOMI over Europe," *Atmospheric Meas. Techn.*, vol. 14, pp. 7297–7327, 2021, doi: 10.5194/amt-14-7297-2021.

[64] D. Frantz et al., "National-scale mapping of building height using Sentinel-1 and Sentinel-2 time series," *Remote Sens. Environ.*, vol. 252, Art. no. 112128, 2021, doi: 10.1016/j.rse.2020.112128.

[65] C. Geiß et al., "Large-area characterization of urban morphology – Mapping built-up height and density with the TanDEM-X mission and Sentinel-2," *IEEE J. Sel. Topics Appl. Earth Observ. Remote Sens.*, vol. 12, no. 8, pp. 2912–2927, Aug. 2019, doi: 10.1109/JSTARS.2019.2917755.

[66] M. Li, E. Koks, H. Taubenböck, and J. van Vliet, "Continental-scale mapping and analysis of 3D building structure," *Remote Sens. Environ.*, vol. 245, 2020, Art. no. 111859, doi: 10.1016/j.eng.2024.01.025.

[67] H. Taubenböck, H. Debray, C. Qiu, M. Schmitt, Y. Wang, and X. X. Zhu, "Seven city types representing morphologic configurations of cities across the globe," *Cities*, vol. 105, 2020, Art. no. 102814, doi: 10.1016/j.cities.2020.102814.

[68] X. X. Zhu et al., "The urban morphology on our planet – Global perspectives from space," *Remote Sens. Environ.*, vol. 269, 2022, Art. no. 112794, doi: 10.1016/j.rse.2021.112794.

[69] J. Voogt, Z. Yuyu, C. Gang, and E. Stokes, "Remote sensing of the urban environment: Beyond the single city, editorial for article collection," 2023. [Online]. Available: https://www.sciencedirect.com/journal/remote-sensing-of-environment/special-issue/10931V8QKZV

[70] L. Dijkstra et al., "Applying the degree of urbanisation to the globe: A new harmonised definition reveals a different picture of global urbanization," *J. Urban Econ.*, vol. 125, 2021, Art. no. 103312, doi: 10.1016/j.jue.2020.103312.

[71] H. Taubenböck et al., "To be, or not to be 'urban'? A multi-modal method for the differentiated measurement of the degree of urbanization," *Comput., Environ. Urban Syst.*, vol. 95, 2022, Art. no. 101830, doi: 10.1016/j.compenvurbsys.2022.101830.

[72] T. Erbertseder, M. Jacob, H. Taubenböck, and K. Zerwer, "How effective are emission taxes for reducing air pollution?," *TRR 266 Accounting for Transparency Working Paper Series No. 114*, Feb. 2023, doi: 10.2139/ssrn.4353315.

[73] V. Shukla and K. Parikh, "The environmental consequences of urban growth: Cross-national perspectives on economic development, air pollution and city size," *Urban Geography*, vol. 13, no. 5, pp. 422–449, 1992, doi: 10.2747/0272-3638.13.5.422.

Thilo Erbertseder received the Diploma degree in geography, with minors in remote sensing and bioclimatology, from the Ludwig-Maximilian University, Munich, Germany, in 1998.

Since 1998, he has been an Atmospheric Scientist and Project Manager with the German Remote Sensing Data Center of DLR, the German Aerospace Center, Wessling, Germany. He has coordinated or participated in more than 50 national and international research projects and has managed large international consortia. He is striving to combine global Earth Observation, urban climate modelling, and health risk assessment to make cities livable, healthy and resilient. His research interests include remote sensing, atmospheric composition research, urban climate change, air quality, and health.

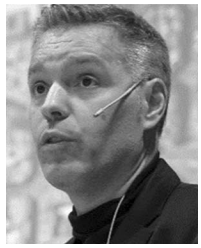

Hannes Taubenböck received the Diploma degree in geography from the Ludwig-Maximilian University, Munich, Germany, in 2004, and the Ph.D. (Dr.rer.nat.) and Habilitation degrees in geography from the Julius-Maximilian University of Würzburg (JMU), Würzburg, Germany, in 2008 and 2019, respectively.

He is currently with the German Aerospace Center (DLR), Wessling, Germany, as well as with JMU. At the German Remote Sensing Data Center (DFD) of the DLR, he heads the department "Georisks and Civil Security," and at JMU, he holds the Chair of "Global Urbanization and Remote Sensing." His research interests include remote sensing topics in the domains of urbanization and risk, from the development of algorithms for information extraction to value adding to classification products for findings in urban geography.

Thomas Esch received the Diploma in applied physical geography from the University of Trier, Trier, Germany, in 2003, and the Ph.D. (Dr. rer. nat.) degree in geography/remote sensing from the Julius-Maximilian University of Würzburg, Würzburg, Germany, in 2006.

In 2023, he was appointed as Honorary Professor at the Faculty of Geomatics, Computer Science and Mathematics, University of Applied Sciences Stuttgart, Stuttgart, Germany. He is a DLR Senior Scientist, Project Manager, and Head of the team "Smart Cities and Spatial Development" with the German Remote Sensing Data Center (DFD), Earth Observation Center (EOC), German Aerospace Center (DLR), Weßling, Germany. He has coordinated or participated in more than 50 international research and development projects, and he is the initiator and main Developer of the Global Urban Footprint (GUF) and the World Settlement Footprint 3D datasets. His research interests include remote sensing, Big Data analytics, and global urban monitoring.

Lorenza Gilardi received the Master of Science degree in environmental and land planning engineering from Politecnico di Milano, Milan, Italy, in 2016. She is currently working toward the Ph.D. degree in geography with the Faculty of Geography, Julius-Maximilian University of Würzburg, Würzburg, Germany.

In 2015, she was a Research Engineer with the Department of Environmental Chemistry, Royal Institute of Technology, Stockholm, Sweden. From 2018 to 2019, she was a scientific employee with the Department of Analytical Chemistry, Technical University of Munich, Munich, Germany. Since 2019, she has been a Researcher with Department "Atmosphere," German Remote Sensing Data Center, German Aerospace Center. Her current research focuses on the effects of environmental stressors on human health, with specific application to urban environments.

Heiko Paeth studied geography, meteorology, and geology at the Rheinische Friedrich Wilhelm University Bonn from 1991 to 1997. He received the Ph.D. degree in meteorology, with a minor in pedology, and the Habilitation degree in meteorology from the Meteorological Institute at the Rheinische Friedrich Wilhelm University Bonn from Meteorological Institute in 2000 and 2005, respectively.

Since 2006, he has been a Professor of physical geography with the Institute of Geography and Geology, University of Würzburg, Würzburg, Germany. His research interests include climate change, and seasonal climate prediction and climate modeling, with regional focuses on Central Europe, the Mediterranean, and Africa.

Stefan Dech received the Diploma, Ph.D., and Habilitation degrees in geography and remote sensing from the University of Würzburg, Würzburg, Germany, in 1987, 1990, and 1997, respectively.

Since 1987, he has been with the German Remote Sensing Data Center of the DLR in various positions, and as Institute Director in 1998. Since 2001, he has been a Professor and Chair of Remote Sensing with the University of Würzburg. Since 2024, he has been a spokesman of the new Earth Observation research cluster at the Institute of Geography and Geology, University of Würzburg. To ensure the practical use of remote sensing products, he is also involved in the development of decision support systems related to natural disasters and the sustainable development of ecosystems. His research focuses on the use of satellite remote sensing for environmental and urban research to enable a better understanding of global change processes.